Behavior of radioactive cesium through the food chain in arthropods and annelids after the Fukushima Dai-ichi nuclear power plant accident

2019

Sota Tanaka

Table of Contents

1. Introduction

1.1 Fukushima Dai-ichi nuclear power plant accident

1.1.1 Main occurrence of the accident

On 11 March 2011, at 14:46 (Japan Standard Time: JST), a massive earthquake with a magnitude of 9.0 occurred on the eastern coast of Japan. The resultant tsunami struck the Fukushima Dai-ichi nuclear power plant (FDNPP), operated by Tokyo Electro Power Company (TEPCO). FDNPP had six units of boiling water reactors, and unit 1, 2 and 3 were in normal operation, while unit 4, 5 and 6 were at various stages of periodic planned refueling and inspection outage (Fig. 1-1) (IAEA, 2015a). Operational reactor units 1-3 were shut down automatically (in a reactor scram) by the earthquake, stopping the nuclear reactions.

The first tsunami wave, with a height of 5.5 m, arrived at 15:27(JST), and the site was effectively protected by its sea wall. However, when the second tsunami wave arrived it had a much larger height of 14-15 m. This second wave passed the seawall and reached the plant, causing units 1-5 to lose all AC power in a station blackout and disabling the reactor cooling system. As a results, the unit 1, 2 and 3 underwent core meltdown, releasing radionuclides into the surrounding environment.

On 12th March at 15:36 a hydrogen explosion occurred in Unit 1 (UNSCEAR, 2013). Meanwhile other events such as vents and explosions continuously occurred in Unit 1-4. Radionuclides were intermittently released into the environment by each of these individual events in each nuclear reactor.

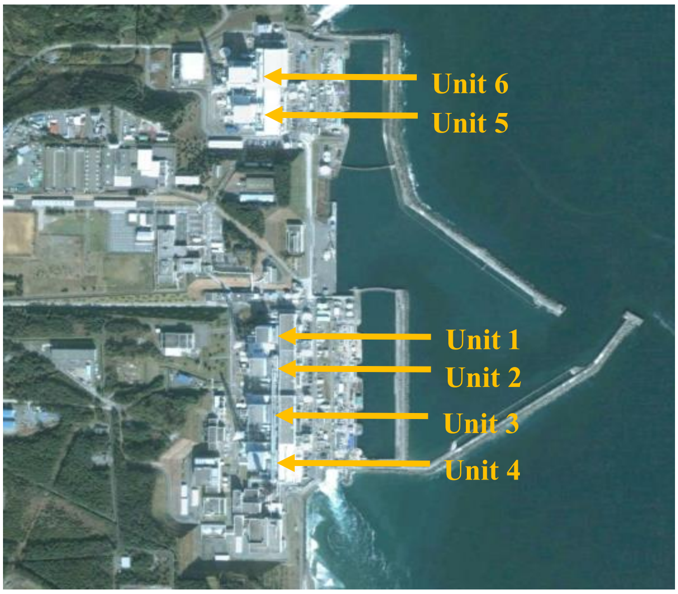

Fig. 1-1 Location of the six units in Fukushima Dai-ichi nuclear power plant (the picture was taken by Google earth in November 21, 2004.)

1.1.2 Amount of radionuclides released

The Fukushima accident was assessed to be level 7 by the estimation of the amount of released radionuclides, the maximum level of the International Nuclear and Radiological Event Scale (INES). Level 7 nuclear accidents have only ever been judged to have occurred at Fukushima and Chernobyl. A comparison of the amount of atmospheric released radionuclides resulting from the Fukushima and Chernobyl accidents is shown in Table 1-1. The amount of radionuclides released in Fukushima was lower than Chernobyl with the exception of ^{133}Xe.

A particularly important released radionuclide in both of these events was radioactive cesium, one of the main fission products. The relatively long half-life of radiocesium (^{134}Cs: 2.06 y, ^{137}Cs: 30.1 y) means that it accumulates in the reactor over time. It also has a comparatively low boiling point, of 671 °C. These properties mean that radiocesium is a dominant radionuclide in atmospheric release and so played a major part in radioactive contamination when the accident occurred. The amount of released radiocesium ($^{134+137}Cs$) in Fukushima was about 25 percent of that released at Chernobyl.

Table 1-1 Amount of atmospheric released radionuclides in the Fukushima and Chernobyl accidents

Radionuclides	Half-life	Amount of radionuclides released (PBq)		Fukushima/ Chernobyl
		Fukushima[a]	Chernobyl[b, c, d]	
Xe-133	5.2 d	11000	6500	1.692
Te-129m	33.6 d	3.3	240	0.014
I-131	8.0 d	160	1760	0.091
Cs-134	2.1 y	18	47	0.383
Cs-137	30.0 y	15	85	0.176
Sr-90	29.1 y	0.14	10	0.014
Zr-95	64.0 d	0.017	84	0.00020
Pu-238	87.7 d	0.000019	0.015	0.00127
Pu-239	24065 y	0.0000032	0.013	0.00025
Pu-240	6537 y	0.0000032	0.018	0.00018

a NISA, 2011

b UNSCEAR, 2008

c Dreicer et al., 1996

d Kashparov et al., 2003

1.1.3 Released radiocesium deposition on the ground

The main release of radionuclides, deposited over a large area of eastern Japan, occurred on 12, 14-16, and 20-23 March (UNSCEAR, 2013). The deposition of radionuclides was determined by meteorological conditions and the characteristics of each release, such as its height and gaseous or particulate form. A major release on 15 March from Unit 2 resulted in wet deposition to the north-east of FDNPP and a high density deposition of radionuclides. The deposition values of ^{131}I, ^{129m}Te, ^{110m}Ag, ^{134}Cs and ^{137}Cs, critical gamma-ray emitting nuclides, was reported (Saito et al., 2015). Of these, ^{131}I, ^{129m}Te, and ^{110m}Ag were dominant for exposure doses in the initial phase after the accident, but low in the longer term due to their relatively short half-lives (^{131}I: 8.0 d,

^{129m}Te: 33.6 d, ^{110m}Ag: 249.9 d). Deposition of ^{238}Pu and $^{239+240}Pu$ was extremely low, being mostly under the detection limit, and ^{89}Sr and ^{90}Sr were significantly lower than the value of ^{137}Cs. The ^{238}Pu, $^{293+240}Pu$, ^{89}Sr, and ^{90}Sr were detected in less than 5% of the area of Fukushima prefecture (UNSCEAR, 2013).

Because of its relatively high deposition and long half-life, radiocesium has been the main source of long-term influence in the environment after the accident. The levels of $^{134+137}Cs$ initial deposition densities on the ground are shown in Fig. 1-2. The highest deposition densities of total radiocesium ($^{134+137}Cs$) in the area north-east of FDNPP were at 3000-30000 kBq/m^2 (Red color area in Fig. 1-2). The area contaminated by more than 555 kBq/m^2 by ^{137}Cs in Fukushima was about 10 % of the area that contaminated by Chernobyl (Imanaka et al., 2015).

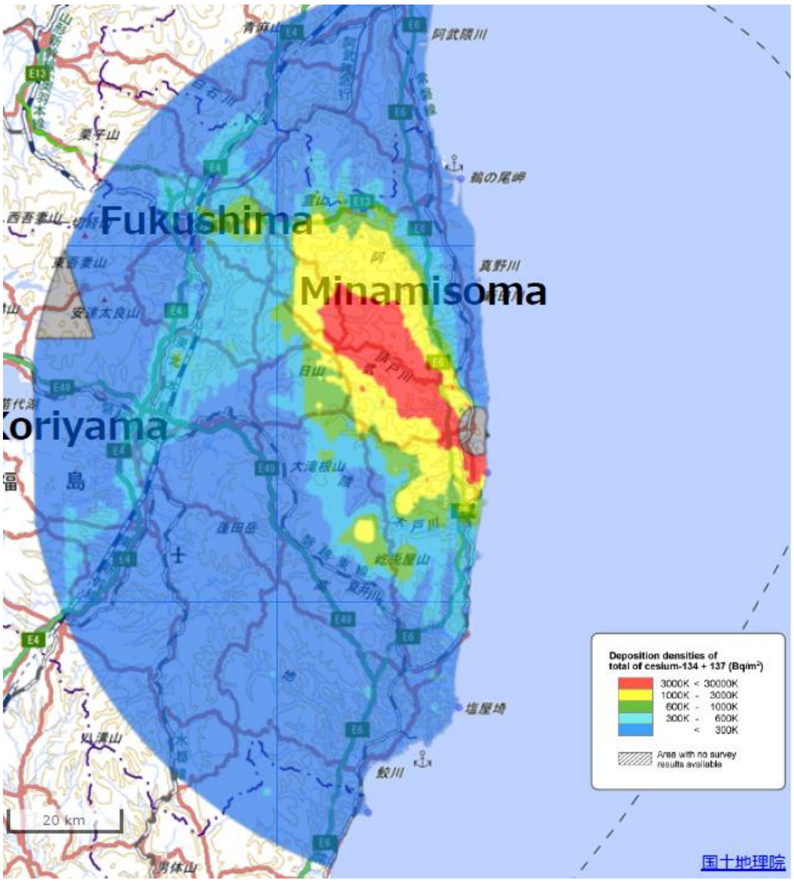

Fig. 1-2 Initial deposition densities of the total radioactive cesium ($^{134+137}Cs$) estimated by airborne survey in April 29, 2011 (MEXT, 2011). (reference figure of the Geospatial Information Authority of Japan was modified.)

1.2 Behavior of radiocesium in the terrestrial ecosystem

1.2.1 Properties of radiocesium

Chemical and physical properties of cesium are similar to its fellow alkali metals, rubidium and potassium. The melting point of cesium is 28.4 °C and its boiling point is 674 °C. Metal cesium is very reactive and causes spontaneous ignition. Cesium ions react with Lewis bases in solution to form complexes and basically forms an ion-binding compound. Cesium has 39 isotopes and its atomic weight is distributed from 112 to 151 (Table 1-2). Cesium-133 is the only stable isotope and is naturally occurring.

Table 1-2 Major* isotopes of cesium

Nuclides	p	n Excitation enegy	Half-life
^{127}Cs	55	72	6.25 h
^{129}Cs	55	74	32.06 h
^{131}Cs	55	76	9.689 d
^{132}Cs	55	77	6.480 d
^{133}Cs	55	78	Stable
^{134}Cs	**55**	**79**	**2.0652 y**
^{134m}Cs	55	138.7441 keV	2.912 h
^{135}Cs	55	80	2.3×10^{6} y
^{136}Cs	55	81	13.16 d
^{137}Cs	**55**	**82**	**30.1671 y**

*Isotopes with half-life of more than 1 hour.

The generation process of radiocesium in the reactor is important. The concentration of ^{235}U in natural uranium is 0.72 %, whereas nuclear fuel rods of the reactor contain 3-5% enriched ^{235}U. When ^{235}U undergoes fission, about 80 kinds of fission products are generated, and the mass number is widely distributed from 72 to 160. These are saddle-shaped distributions centered on the peaks around the mass numbers 90 and 140. Strontium ($^{89+90}$Sr) within the range of peak mass numbers has high fission yield at total 10.5 %, but the boiling point of strontium is 1382°C and the value is two times higher than cesium. Therefore, cesium is more easily released than strontium into the atmosphere in the accident. Cesium-135 is a long-lived fission product (Half-life: 2.3×10^{6} y), however, its precursor of ^{135}Xe absorbs neutrons and decreases fission response or converted to nonradioactive ^{136}Xe. Therefore, ^{135}Cs is not major fission products in the reactor. The direct generated fission yield of ^{137}Cs in thermal neutron nuclear fission is only 0.06 %, however, the short half-life of other fission products such as ^{137}I, ^{137}Xe, and ^{137}Te beta-collapsed to ^{137}Cs and total fission yield of ^{137}Cs is 6.19 % (Table 1-3). Cesium-134 has a lower direct generated fission yield at 4.4×10^{-6} %, however, neutron capture reaction (^{133}Cs (n, γ) ^{134}Cs) occurred in the reactor and the total fission yield of $^{133+134}Cs$ is 6.79 % (England and Rider, 1995). Consequently, $^{134+137}Cs$ was the main releasable radionuclide into the atmosphere in the accident.

Table 1-3 Major fission products and fission yield of ^{235}U

Fission products	Fission yield	Half-life
^{133}Cs	6.70%	Stable
^{135}I	6.28%	6.57h
^{93}Zr	6.30%	1.53My
^{137}Cs	**6.19%**	**30.17y**
^{99}Tc	6.05%	211ky
^{89}Sr	4.73%	50.53d
^{90}Sr	**5.75%**	**28.9y**
^{131}I	**2.83%**	**8.02d**
^{147}Pm	2.27%	2.62y
^{149}Sm	1.09%	Stable
^{129}I	0.54%	15.7My
^{133}Xe	6.70%	5.2475d

Due to the nuclear accident radiocesium was released into the atmosphere in the form of aerosol. In previous studies, the initial chemical form of radiocesium released into the atmosphere after an accident was identified as CsOH or CsI (Auvinen et al., 2000). In the FDNPP accident, initial released CsOH or CsI particles were incorporated with the sulfate aerosol (Kaneyasu et al., 2012). The particle size at 0.1-2 μm of sulfate aerosol would have been transported long distances in the atmosphere and fall by dry and wet deposition on the environment. Insoluble radiocesium particles were also found in the aerosol after the FDNPP accident (Adachi et al., 2013). Therefore, radiocesium released into the atmosphere in FDNPP accident came in both soluble and insoluble forms.

The released radiocesium was deposited on the terrestrial environment surrounding Fukushima. Cesium is homologous element of potassium, an essential element for living organisms. Because of this, radiocesium can enter food webs and circulate in the ecosystem over the long-term. Combined with the relatively long half-life of radiocesium (^{134}Cs: 2.06y, ^{137}Cs: 30.1 y), $^{134+137}$Cs became the main contaminating nuclides in the environment after the accident.

1.2.2 Geological and ecological characteristics of Fukushima prefecture

Fukushima Prefecture is covered with 974,000 ha of forest, 58.1 % are private forests and 41.9% national forests (Fukushima Prefectural Government, 2017). The total forest area accounts for 71% of the total land area of the prefecture. The forests in Fukushima are dominated by deciduous broad-leaved trees and laurel trees, with tree distribution varying by altitude. At over 1,500 m altitude the subalpine belt is dominated by *Abies mariesii*, which have a lower limit of distribution at an altitude of 400m (700-800m is the lower limit in the Ōu moutains and the Abukuma area). The upper montane zone, up to 1,500m, is dominated by *Fagus crenata*, the lower montane zone, up to 1,500 m, is dominated by *Quercus serrata*, and the lowland zone, at less than 400-500 m is dominated by *Castanopsis* trees (Kashimura, 1984). In practice the actual vegetation is more complicated, depending on geological and topographical conditions. Land use of Fukushima prefecture mainly forest and an estimated 82% of the prefectural area is hilly and mountainous regions, which is surrounded by forest (Fukushima Prefectural Government, 2010).

Because of this large cover of land by forest and the relatively high attachment of radioactive aerosol particles onto the surface of trees, there was a heavy deposition of released radiocesium forested areas. The land use of hilly and mountainous regions comprises a mosaic distribution of forestry area, farmland, paddy field, pasture land and residential areas. The composition of the biota and nature of the ecosystem in these hilly and mountainous areas is dependent on this land use. These ecosystems have been contaminated by radiocesium, and a long-term influence is feared. The total area of evacuation designated zones is 371 km^2 and more than 44,800 people remain evacuated in 2018 (Fukushima Prefectural Government, 2018).

1.2.3 Previous study of radiocesium in the terrestrial ecosystem

Environmental contamination with radiocesium was observed after the Chernobyl accident (Cort et al., 1998). Large land areas 57900 km^2 in Russia, 46500 km^2 in Belarus, and 41900 km^2 in Ukraine were contaminated by ^{137}Cs over 37 kBq/m^2, equating to 1 mSv per year when external exposure and effects of radiation are considered (IAEA, 2006). Some areas of other countries such as Sweden, Finland, Austria, Norway, Bulgaria, Switzerland, and Greece etc. were also contaminated. The environmental behavior of radiocesium and its possible effects on human and ecosystem had been summarized elsewhere (UNSCEAR, 1988; UNSCEAR, 2000; WHO, 2006; IAEA, 2006; UNSCEAR, 2008; UNSCEAR, 2013; IAEA, 2015a; IAEA, 2015b; WHO, 2016).

Radiocesium derived from FDNPP was initially deposited on the forest-floor or forest canopies and accumulated further on the forest floor via throughfall, litterfall, and stemflow processes (Koarashi et al., 2012; Kato et al., 2012; Teramage et al., 2014; Loffredo et al., 2014). It is maintained in the long-term on the soil surface due to having been strongly adsorbed by soil minerals. The annual vertical migration of ^{137}Cs to a depth of 10 cm in the soil only accounts for 0.1% of the total ^{137}Cs inventory (Nakanishi et al., 2014). As a result, a large part of the radiocesium accumulated on the soil surface layer in the long-term. The radiocesium circulates in the forest ecosystem via biological cycles such as reabsorption by trees (Goor and Thiry, 2004; Thiry et al., 2016; Yoshihara, 2017; Kato et al, 2018), retention by fungi (Steiner et al., 2002; Vinichuk et al., 2004), and direct ingestion and/or assimilation by animals through the food webs (Allaye-Chan et al., 1990; Kålås et al., 1994). This means that bioavailability of radiocesium is maintained, and could be transferred between organisms in the long-term through the food web. Therefore, to understand the long-term behavior of radiocesium in the ecosystem, the transfer and circulation of radiocesium through the food web is important. However, the study of radiocesium behavior in the food web to date has been insufficient, in a large part due to the difficulty of long-term investigation in wildlife.

1.3 Objectives and structure of this study

The objectives of this study are to understand the long-term behavior of radiocesium in the ecosystem through the terrestrial food web. To accomplish this, we focused on terrestrial invertebrates such as arthropods and annelids (earthworms). The field survey was conducted in Fukushima after the accident and chronological changes of radiocesium in different feeding habit of arthropods and earthworms were investigated from 2012 to 2016.

In Chapter 2, the concentration of radiocesium in three species of arthropods and ambient dose equivalent rates of sampling sites was investigated after the accident. Five-year chronological changes of radiocesium in different feeding habit of arthropods were provided.

In Chapter 3, the concentration of radiocesium in epigeic earthworms was investigated from 2014 to 2016, as well as ambient dose equivalent rates. The concentration of radiocesium in the different feeding habits of arthropods and earthworm were compared as herbivores, omnivores, carnivores and detritivores.

In Chapter 4, radiocesium distribution in the earthworm body was visualized by autoradiography. To understand the metabolism of radiocesium in the earthworms, the retention time of radiocesium was investigated in the laboratory and the biological half-life of radiocesium was determined.

In Chapter 5, to evaluate radiation effects on arthropods and earthworms, the absorbed dose rate was estimated. The radiation risk on arthropods and earthworms was discussed.

Finally, in Chapter 6, the environmental behavior of rasiocesium through the food chain and radiation risk on non-human species were discussed.

2. Chronological changes in the concentration of radiocesium in arthropods

2.1 Background and objectives of the study

The objective of this study was to understand the long-term behavior of radiocesium in the ecosystem through the terrestrial food chain. For this, long-term and comprehensive investigation of radiocesium at each trophic level of organisms is necessary. Suitable selection of the indicator organism is therefore essential in this type of study. It is difficult to conduct long-term and stable research into animal group including higher trophic level species such as mammal, and birds; selecting these groups as indicator carnivores requires long-term and constant sampling, which is time and cost consuming. Moreover, the sampling process could have a negative impact on the food web structure due to sampling a small number of top predators.

The kingdom Animalia is known to represent a total of 1,552,319 species in 40 phyla according to a new evolutionary classification, and the phylum Arthropoda alone represents 1,242,040 species, which is approximately 80% of the total (Zhang, 2011). Arthropods are the most successful organism group. They have a large biomass, universal distribution, and various feeding habits in the ecosystem, and are important food sources for other organisms. The characteristics of arthropods enable their long-term study as indicators of radiocesium through the food chain.

In this study, to understand the chronological changes of radiocesium in arthropods from different feeding habits, five-year field studies were conducted in Fukushima. Three species of arthropods were selected: rice grasshopper, field crickets, and web-making spiders, which are common species in hilly and mountainous areas. The radiocesium concentrations in these arthropods and the ambient dose equivalent rates at the sampling site were investigated from 2012 to 2016.

2.2 Materials and methods

2.2.1 Sampling site

The sampling site is located 40.1 km northwest of FDNPP (latitude: 37°41′35″ N, longitude: 140°44′08″ E; Fig. 2-1). The deposition densities of total radiocesium ($^{134+137}Cs$) at the sampling site in 2012 estimated from an air born monitoring survey were 1000-3000 kBq/m^2 (MEXT, 2011). The landscape of the sampling site is hilly and mountainous area, with an altitude of approximately 440–480 m, and composed of agricultural fields and residential areas surrounded by mountainous forest. Residents were not permitted to live in this area during the study period from 2012 to 2016. Sampling was conducted in the same area throughout all five years of the study.

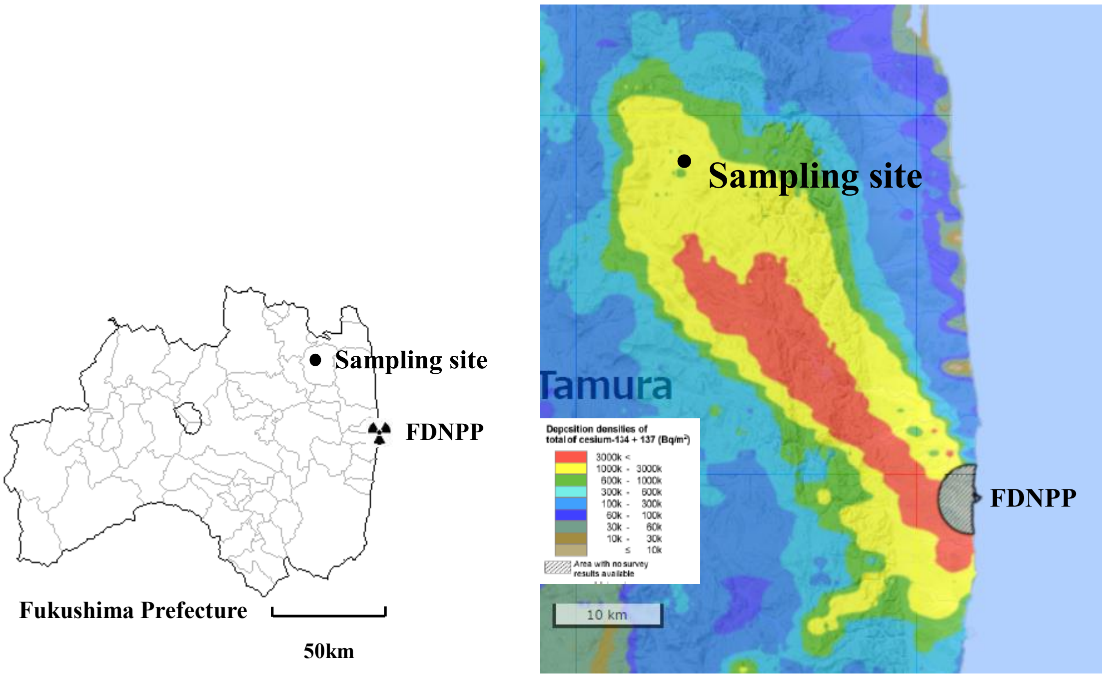

Fig. 2-1 Location and deposition densities of radiocesium on 28 June 2012, at the sampling site (MEXT, 2011). Fukushima Dai-ichi nuclear power plant is indicated by FDNPP. (reference figure of the Geospatial Information Authority of Japan was modified.)

2.2.2 Ambient dose equivalent rates

Ambient dose equivalent rates are attributed to gamma rays from the ground; thus, they are an indicator of radioactive contamination in the environment. A NaI scintillation survey meter (TCS171, Hitachi, Ltd., Japan) was used to measure the ambient dose equivalent rate at the sampling site. The calibration performed with the replacing method of JIS Z 4511-2005, using the working standard instruments (JCSS) irradiation apparatus calibrated by Hitachi Aloka Medical, Ltd. on November 18, 2011. Measurements were conducted at multiple points within the sampling site, 1 m above the ground and at least 20 m apart.

To estimate the weathering of radiocesium from the sampling site, the ambient dose equivalent rates were compared to the estimated ambient dose equivalent rates from the physical half-life of radiocesium (^{134}Cs: 2.06y, ^{137}Cs: 30.1 y). For physical decay correction of ambient dose equivalent rates, the contribution ratio of ^{134}Cs and ^{137}Cs to the ambient dose equivalent rates were calculated using a conversion factor (IAEA, 2000), which assumed that the radiocesium was uniformly distributed on the ground. The activity ratio of ^{134}Cs/^{137}Cs was set at 1.0 at the time of the accident.

2.2.3 Sampling of arthropods

The sampling was conducted from September to October each year between 2012 and 2016 (Fig. 2-2). The rice grasshopper, *Oxya yezoensis* Shiraki (Orthoptera: Catantopidae), the Emma field cricket, *Teleogryllus emma* (Ohmachi et Matsuura) (Orthoptera: Gryllidae), and the Jorô Spider, *Nephila clavata* L. Koch (Araneae: Nephilidae), were collected by sweep-net and hand collection. For each arthropods, 20–200 individuals were collected

Fig. 2-2 Sampling site of arthropods (11 Sep. 2014)

each year. The collected arthropods were preserved immediately in 70% ethanol in the field and refrigerated until sorted.

2.2.4 Measurement of radiocesium concentration in arthropods

Radioactivity in the arthropod samples was measured by gamma-ray spectrometry using a high-purity germanium detector (GC-2020, Canberra Industries and GEM30-70, ORTEC, USA) with a multi-channel analyzer (MCA: DAS1000, Canberra Industries and Easy-MCA-8k, ORTEC, USA). The counting efficiency of the detector was determined by measuring a certified mixed radioactive standard gamma volume source (MX033SPLU8, Japan Radioisotope Association and 24FY039, Japan Chemical Analysis Center). Samples of 10–50 individuals were placed into 100-ml plastic containers (U-8 container) and measured for 3,600–10,800 s. The radioactivity of the samples was obtained in units of Bq/g fresh weight (Bq/g fw).

2.2.5 Statistical analyses

The lower (Q1) and upper (Q3) quartiles and the interquartile range (IQR = Q3–Q1) were calculated for changes in the radiocesium concentration in arthropods. Differences in the values between years were analyzed by the Kruskal–Wallis test. Spearman's rank correlation was used to test the relationship between the ambient dose equivalent rates and the concentration of radiocesium in the arthropods. Statistical analyses were performed using R version 2.15.3 (R Core Team, 2013).

2.3 Results

2.3.1 Ambient dose equivalent rates at the sampling site

The ambient dose equivalent rate at the sampling site is plotted with circles in Fig. 2-2. The median ambient dose equivalent rates differed significantly with time after the accident (Kruskal–Wallis test, $p < 0.05$). Multiple comparisons by Scheffe's method indicated that the values decreased significantly from 2012 to 2015 ($p < 0.05$) with no significant decrease from 2015 to 2016. The median ambient dose equivalent rates decreased from 3.74 μSv/h to 1.29 μSv/h in the five-year period between 2012 and 2016. The decrease of median values during the initial phase of the survey period from 2012 to 2013 was 29% whereas that in the later phase from 2015 to 2016 was only 4%. The total reduction in the median ambient dose equivalent rate during the survey period from 2012 to 2016 was calculated as 65%.

The decline of ambient dose equivalent rates estimated due to the physical decay of ^{134}Cs and ^{137}Cs is plotted with a dotted line in Fig. 2-3. The estimated values were 2.62 μSv/h, 2.0.1 μSv/h, 1.66 μSv/h, and 1.46 μSv/h from 2013 to 2016, respectively (Table 2-1). The actual ambient dose equivalent rates at the sampling site fit with the estimated values from the initial year until 2014 then became slightly lower than the estimated rates in 2015 and 2016.

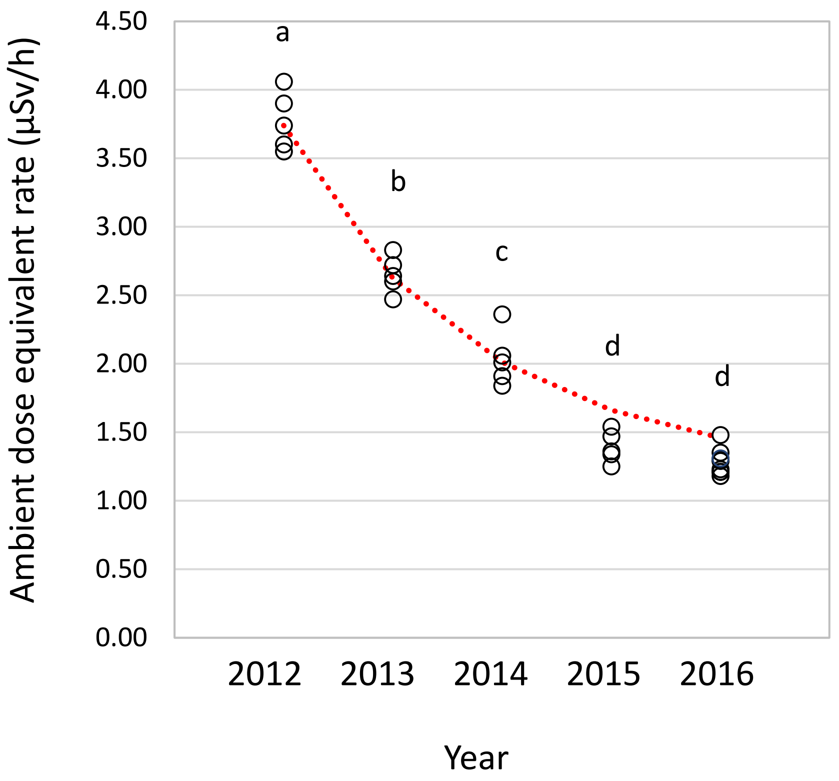

Fig. 2-3 Chronological changes in ambient dose equivalent rates at the sampling site compared to the estimated decline of ambient dose equivalent rates due to the physical decay of radiocesium (dotted red line). Letters above the plots denote significant differences in multiple comparisons by Scheffe's method ($p < 0.05$).

Table 2-1. Median value of measured ambient equivalent dose rates and estimated value due to the physical decay of radiocesium.

µSv/h	2012	2013	2014	2015	2016
Measured value	3.74	2.64	2.01	1.36	1.29
Estimated value	3.74*	2.62	2.01	1.66	1.46

* The measured value is used at initial value to estimate ambient dose equivalent rates due to the physical decay of radiocesium.

2.3.2 Chronological changes in the concentration of radiocesium in arthropods

Chronological changes of radiocesium concentration in arthropods are shown in Fig. 2-4. The median concentration of radiocesium in rice grasshoppers was significantly reduced from 0.46 to 0.05 Bq/g fw between 2012 and 2016 (Kruskal–Wallis test, $p < 0.05$; Fig. 2-4 (A)). A significant decrease of radiocesium concentration also occurred in field crickets, with values from 0.15 to 0.01 Bq/g fw between 2012 and 2016 ($p < 0.05$; Fig. 2-4 (B)). In contrast, the Jorô spider showed no significant differences during the sampling period ($p = 0.14$, Fig. 2-3 (C)); the median radiocesium concentration from 2012 to 2016 was 0.31, 0.33, 0.20, 0.23, and 0.14 Bq/g fw, respectively.

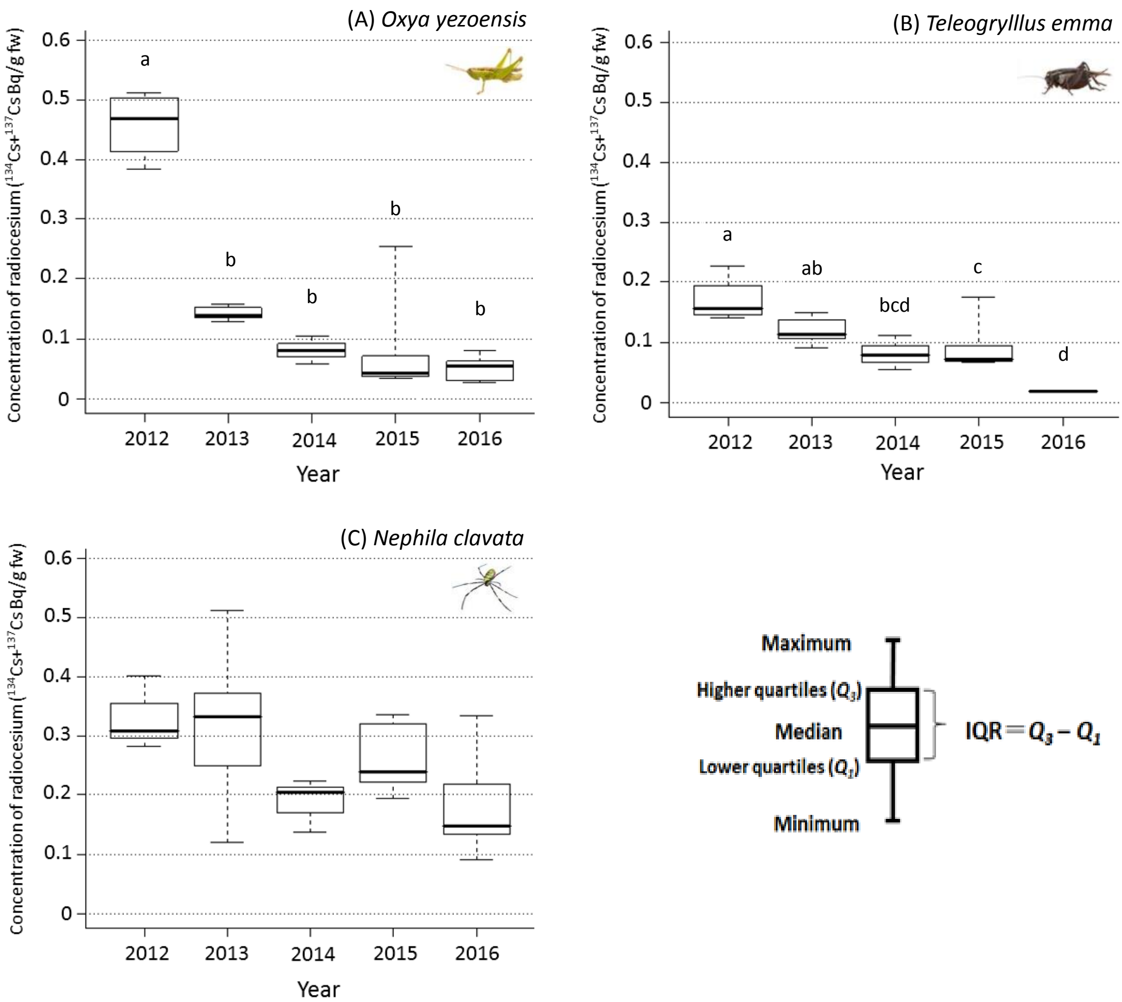

Fig. 2-4 Chronological changes of radiocesium concentration in arthropods: (A) *Oxya yezoensis*, rice grasshopper, (B) *Teleogryllus emma*, field cricket, and (C) *Nephila clavata*,

Jorô spider. Minimum and maximum concentrations are depicted by whiskers. The box signifies the upper and lower quartiles, and the median is represented by a horizontal line within the box for each year. Different letters above the box plots denote significant differences in multiple comparisons by Scheffe's method ($p < 0.05$).

2.3.3 Correlation between the ambient dose equivalent rates and radiocesium concentration in arthropods

The strength of the relationship between the ambient dose equivalent rates and the concentration of radiocesium in the arthropods was analyzed from 2012 to 2016 (Fig. 2-5). A significant positive correlation ($p < 0.05$) was observed in the rice grasshoppers, the Emma field crickets and the Jorô spiders. The highest correlation coefficient was observed in the grasshoppers (ρ = 0.852), followed by the field cricket (ρ = 0.808) and the spider (ρ = 0.509).

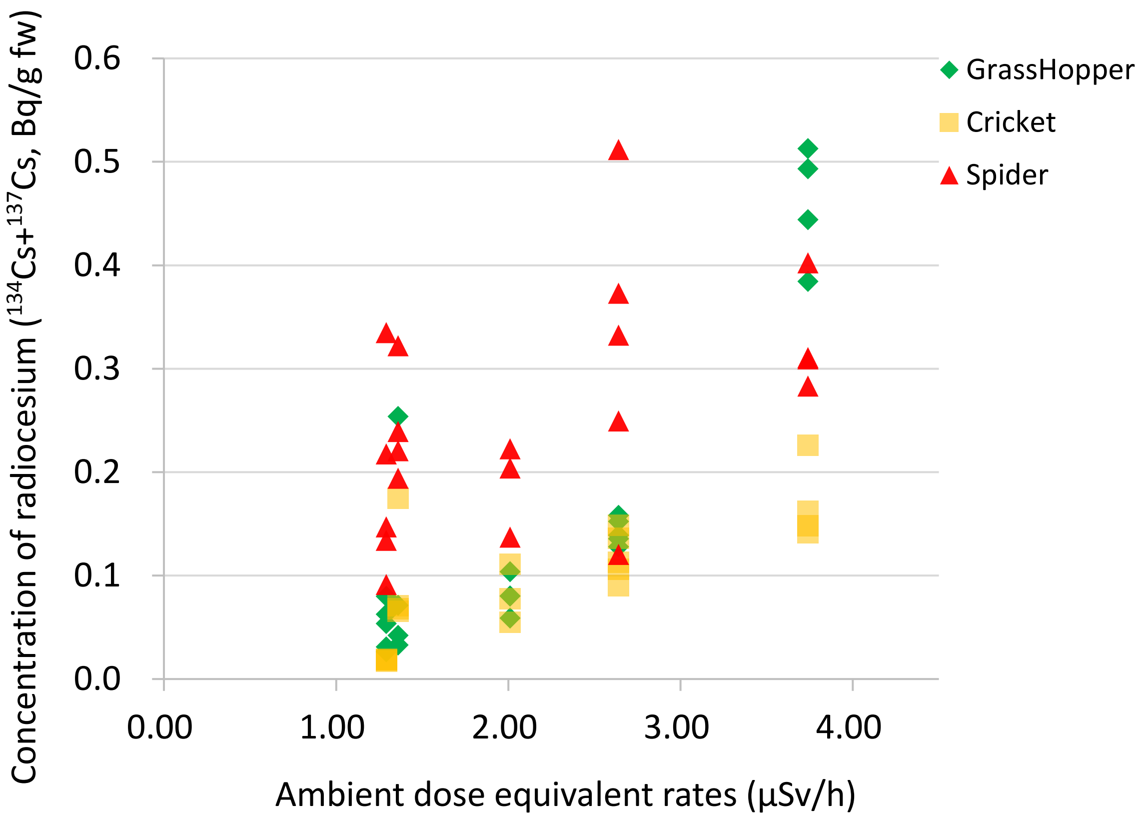

Fig. 2-5 Correlation between ambient dose equivalent rates and radiocesium concentration in the arthropods. Diamonds, squares, and triangles represent the rice

grasshopper, the Emma field cricket, and the Jorô spider, respectively. The Spearman's rank correlation coefficient (ρ) and p value for the arthropods are as follows: rice grasshopper: $\rho = 0.852$, $p < 0.001$; Emma field cricket: $\rho = 0.808$, $p < 0.001$; Jorô spider: $\rho = 0.509$, $p = 0.018$.

2.4 Discussion

2.4.1 Ambient dose equivalent rates

The decline of ambient dose equivalent rates in the environment, known as the "ecological half-life", depends on the physical decay and weathering of radiocesium. The decline curve of ambient dose equivalent rates due to physical decay was calculated by differences in the contribution ratio of ^{134}Cs and ^{137}Cs to the ambient dose equivalent rates (Saito and Petoussi-Henss, 2014). With an assumed the activity ratio of $^{134}Cs/^{137}Cs$ of 1.0, according to the average ratio of radiocesium released from Fukushima reactor plants 1–3, the contribution ratio for ambient dose equivalent is approximately 7:3 for ^{134}Cs and ^{137}Cs, respectively. Cesium-137 emits 662 keV gamma rays at a rate of 85% during a decay, while ^{134}Cs emits multiple gamma rays from 600–1,370 keV at a total rate of 200% during decay. Therefore, ^{134}Cs contributes more to the ambient dose equivalent rates than ^{137}Cs. The half-life of ^{134}Cs (2.06 y) is shorter than that of ^{137}Cs (30.1 y); thus, the contribution ratio of ^{134}Cs decreases each year. Therefore, the ambient dose equivalent rates the first initial year after the accident decreased rapidly due to the physical decay of ^{134}Cs then decreased slowly due to the physical decay of ^{137}Cs. The weathering of runoff and/or downward migration of radiocesium from the surface of the soil also leads to a decrease in the ambient dose equivalent rate in the environment. Consistent decreases in these factors were observed at the sampling site.

The ambient dose equivalent rates decreased significantly and constantly from 2012 to 2015, but no significant decrease was observed from 2015 to 2016. During the initial years from 2012 to 2014, the ambient dose equivalent rates is closely fitted the decline curve of the physical decay of radiocesium (Fig. 2-3; Table 2-1). This indicates that temporal changes in the ambient dose equivalent rates were predominantly attributable to the physical decay of radiocesium, and the weathering of radiocesium from the sampling site was relatively minimal from 2012 to 2014. From 2015 to 2016, the ambient dose equivalent rates were slightly higher than the decline curve. This suggests that runoff and/or downward migration of radiocesium from the sampling site occurred but to a small extent.

2.4.2 Chronological changes in the concentration of radiocesium in arthropods

The chronological changes of radiocesium concentration were different in each type of arthropods. Although the median radiocesium concentration in grasshoppers and field crickets changed significantly from 2012 to 2016, no significant decrease of radiocesium concentration was observed in Jorô spiders. These differences likely attribute to the different food resource pathways of thier feeding habits from grazing and detrital food chain (Polis and Strong, 1996). High ^{137}Cs concentrations in detritivore groups suggest that the ^{137}Cs transferred between organisms flows up to higher trophic levels through the detritus food chain (Murakami et al., 2014). Grasshoppers rely on the grazing food chain, feeding exclusively on green plants, while field crickets and web spiders make use of both of the food chains (ElEla et al., 2010; Simazaki et al., 2005).

The radiocesium in grasshoppers decreased rapidly from 2012 to 2013 and the values remained low from 2013 to 2016. The rice grasshopper is polyphagous but known to predominantly eat Poaceae plants such as rice; thus, they are one of most abundant pests in paddy fields (Ando and Yamashiro, 1993; Mitsuhashi, 2003). EIEla et al. (2010) analyzed the gut contents of orthopteran species in Japan and classified seven groups as follows: Herbivorous (H), Herbivorous with scavenging behavior (H_s), Graminivorous (G), Forbivorous (F), Forbivorous with scavenging behavior (F_s), Scavengers (S), and Predators (P). The grasshopper, *Oxya yezoensis*, was categorized as Graminivorous (G), where the number of fragments of monocotyledonous species is more than 75% of the gut contents.

The transfer of radiocesium to plants has two pathways: uptake by direct deposition of radiocesium on the leaf and uptake through roots from soil to plants (Tagami, 2012). Leaf uptake depends on radiocesium concentration in the atmosphere; thus, the contribution of root uptake increases with time after the accident. In Poaceae plants, the main food of grasshoppers, most parts of the plant are annual plants and wither in winter. Moreover, these plants were likely in the growth stage of seed or rhizome when the accident occurred in March. This field study was conducted in 2012, the radiocesium in these plants was mainly taken up by the roots. Therefore, the grasshoppers mainly ate leaves contaminated by absorption from the roots during the sampling period.

Radiocesium in soil is known to be immobilized by soil clay minerals (Nakao et al., 2008); thus rapidly decreases the bioavailability of radiocesium (Takeda et al., 2013). Regarding the transfer of radiocesium from soil to grass after the Chernobyl nuclear accident, it was reported that the bioavailability of radiocesium decreased rapidly in the initial year from 1987–1989, with half-lives of 1.3–2.6 years, then decreased more slowly 1989–1999, with half-lives of 4.6–21 years (Fesenko et al., 2009). In this study, radiocesium concentrations in grasshoppers decreased rapidly in the initial year from 2012–2013 and remained low level from 2013–2016. These results are consistent with chronological changes in radiocesium concentrations in plants after the accident. Radiocesium concentrations in grasshoppers refrect the concentration of Poaceae annual plants. Due to the above reasons, radiocesium concentrations in grasshoppers would remain low in the long-term.

The radiocesium in field crickets also decreased significantly from 2012 to 2016, but the initial value in 2012 was lower than that of grasshoppers. Due to thier feeding habits, field crickets were categorized as Scavengers (S), where roots or tubers of plants and dead orthopteran and /or oligochaetan parts are encountered in almost equal proportions (ElEla et al., 2010). Crickets have a particularly high ability to feed on a large variety of weed seeds (Carmona et al., 1999; Lundgren and Rosentrater, 2007). The field criket, *Teleogryllus emma*, adults occur from August to October after the seed-shedding and they have also capable of feeding on seeds and reducing the seedling emergence of weeds (Ichihara et al., 2012). Weed seeds are one of the most accessible food resource for field crickets.

The transfer factor of radiocesium in various wild weeds in the initial year after the FDNPP accident showed large variation from 0.006-0.400 (Yamashita et al., 2014). Radiocesium had high bioavailability in initial year; thus, variations in the transfer factor became high. The difference in 2012 radiocesium concentrations between grasshoppers and field crickets can be explained by the bioavailability of plant and feeding preference of each arthropod. The chronological changes of radiocesium in grasshoppers and field crickets were approximately the same from 2013 to 2016. This is consistent with a previous study of radiocesium bioavailability in grasses after the accident. This suggests that the field crickets mainly feed from the grazing food chain.

The concentration of radiocesium in Jorô spiders has a larger dispersion and is maintained at higher concentrations than other arthropods. This may be because web spiders such as the Jorô spider are known to prey from both grazing and detiritus food chain as a generalist predator (Shimazaki and Miyashita, 2005). This study shows that the radiocesium in grasshoppers feeding from the grazing food chain was low from 2013 to 2016. This suggests that radiocesium concentrations in Jorô spiders become low when they prey from the grazing food chain. In contrast, radiocesium concentrations in Jorô spiders would be high when they prey from the detritus food chain. This is because detritivores consume highly contaminated leaf litter that cascade up through detritus food chain (Polis and Strong., 1996). Ayabe et al. (2015) reported that the radiocesium contamination in the Jorô spider decreased from 2012 to 2013, but highly contaminated spiders (> 9.0 Bq/g dry) were still collected in 2013. In this study, no significant decrease was observed during the five-year period. This is likely because web-making spiders such as the Jorô spider rely more on prey such as saprophagous flies for their food resource than herbivores (Miyashita et al., 2003); i.e., they feed more from the detritus food chain.

2.4.3 Correlation between ambient dose equivalent rates and radiocesium concentration in arthropods

A significant correlation between ambient dose equivalent rates and radiocesium concentrations was observed in all arthropods. A particularly high correlation coefficient was observed for the rice grasshoppers (ρ = 0.852) and field crickets (ρ = 0.808). The two species depend on plants; solely for the grasshoppers and for at least half of the cricket's food source. The flying ability of these two species is also minimal. The collected grasshoppers were short-wing type (brachypterous), which either do not fly or only fly for a few meters (Ando, 1996). In fact, no flying grasshopper individuals were observed at the sampling site; they only jumped using their hind legs. The field crickets lived on/in the ground and again, no flying individuals were observed at the sampling site. The dispersion ability of the two species was therefore low so their food resource was likely located near the sampling site.

The correlation coefficient between ambient dose equivalent rates and radiocesium concentrations for the Jorô spider was lower (ρ = 0.509) than the other two species. The juveniles of *Nephila* spiders, which are smaller than 1 mm, are easily dispersed by ballooning behavior (Robinson and Robinson, 1973; Kuntner and Agnarsson, 2011). In this study, the spiders were collected in female adult stage; thus, their dispersal abilities would be relatively low. However, web-building spiders such as *Nephila clavata* prey on a large variety of aerial insects as a generalist predator (Shimazaki and Miyashita, 2005). Moreover, they depend on detritivores that emerge from under the ground (Miyashita et al., 2003). Therefore, the spiders feed from a wider area than the other two species and may consume highly contaminated prey from under the ground through the detritus food chain. The concentration of radiocesium in Jorô spiders therefore reflects wider area of contamination, which could explain the lower correlation coefficient.

3. Chronological changes in radiocesium concentrations in epigeic earthworms

3.1 Background and objectives of the study

As described in the previous chapter, results pertaining to chronological changes in radiocesium concentrations in arthropods suggested that the primary transfer pathway of radiocesium is the detritus food chain. If radiocesium transfers to other species through the detritus food chain, the radiocesium concentration in detritivores should be maintained at higher levels than species with alternative feeding habits. To evaluate this hypothesis, the investigation of the concentrations of radiocesium in detritivores is necessary.

Earthworms contribute to the disturbation of soil acting as ecosystem engineers (Lavelle et al., 1997) and are an important food resource for higher trophic consumers such as arthropods, birds, and mammals, among others. These ecological activities of earthworms can contribute to the circulation of radiocesium in the soil and its transfer to organisms through the food web.

Earthworms can be subdivided into three ecological groups (Bouché, 1977; Lee, 1985): epigeic (inhabiting the litter layer), anecic (inhabiting soil and feeding on litter), and endogeic (inhabiting and feeding on soil). Epigeic earthworms that live in the litter layer and the soil surface layer are an important ecological group in regard to the behavior of radiocesium, which mostly accumulates in the ground surface layer. Hasegawa et al. (2013) conducted a field study of different species of epigeic earthworms in Fukushima and reported that earthworms from the epigeic group have similar radiocesium concentrations because of their similar habitats and physiological characteristics. In the present study, therefore, we focused on epigeic earthworms at the family level to understand the behavior of radiocesium through the detritus food chain.

A field study conducted to assess the effects of radiation on non-human biota after the Chernobyl accident found catastrophic effects on soil invertebrate communities including earthworms (IAEA, 2006). Soil invertebrates had higher absorbed dose rates than other animals because their habitats were highly contaminated. The population densities and species diversity of soil invertebrates were decreased in Chernobyl with an absorbed dose higher than approximately 30 Gy; the population densities of earthworms, in particular, decreased due to their high radio-sensitivity during the egg and juvenile stages (Krivolutzkii et al., 1992). These results indicate that earthworms are a susceptible species to the effects of radiation after nuclear accidents. Given that, the International Commission on Radiological Protection selected the earthworm as a reference animal to assess the effects of radiation on the environment (ICRP, 2008).

Earthworms are an important species for predicting the long-term environmental behavior of radiocesium and assessing the effects of radiation on non-human species. Therefore, the present study was designed to assess the chronological changes in radiocesium concentrations in epigeic earthworms from the mountainous forests of Fukushima. We conducted a field survey in Fukushima and compared the chronological changes in radiocesium levels in earthworms, litter, soil, and the ambient dose equivalent rates from 2014 to 2016.

3.2 Materials and methods

3.2.1 Sampling site and measurement of ambient dose equivalent rates

The sampling site was a hilly and mountainous area on the forest side of the same region described in section 2.2.1. The sampling site is a mixed forest dominated by deciduous broad-leaved trees. Residents were not permitted to live in this area, and decontamination operations had not been conducted prior to or during the study period from 2014 to 2016.

The earthworm sampling site was different from where arthropods were collected, so ambient dose equivalent rates were measured using the same methods as described in 2.2.2.

3.2.2 Sampling and pretreatment of soil, litter, and earthworms

The sampling of earthworms was carried out within a radius of approximately 30m (an area of ca. 2800 m^2) and was repeated at the same site throughout the three years of the study. In addition, soil and litter were also collected at the same site. Epigeic earthworms were collected by hand from the litter layer and soil surface (≤5 cm) from August to September (Fig. 3-1). The earthworms were identified as belonging to the family Megascolecidae based on external morphology, particularly the clitellum, and the internal morphology was assessed by dissecting several representative individuals (Fig. 3-2). There were 1, 5, and 5 earthworms in each of the five samples taken from 2014, 2015, and 2016, respectively; thus, a total of 5, 25, and 25 individuals were collected, respectively, during those years. The soil was collected at depths of 0–5 cm using a core sampler (50mm in diameter, 51mm high), and litter was sampled in a 25 cm×25 cm area of the forest floor. The number of soil and litter samples taken in 2014, 2015 and 2016 were 1, 3, and 3, respectively. After being oven dried at 105°C, the soil was sifted through a 2 mm square mesh, and the litter was homogenized in a blender.

The concentrations of ^{137}Cs in the earthworms were determined from the measured radioactivity that included the contents of the gut, since predators would consume the entire body of the earthworm (Sheppard et al., 1997); this method is therefore appropriate for understanding how radiocesium is transferred through the food web.

Fig. 3-1 Sampling of the epigeic earthworms (11 Sep. 2014)

Fig. 3-2 Epigeic earthworm (Megascolecidae) (29 Aug. 2016)

3.2.3 Measurement of radiocesium in samples

All samples were packed into plastic containers (U-8: 47mm diameter, 60mm in height). The activity of ^{137}Cs (662 keV) was determined by gamma-ray spectrometry using a high-purity germanium detector (GEM30-70, ORTEC, USA) with a multi-channel analyzer (Easy-MCA-8k, ORTEC, USA). The counting efficiency of the detector for U-8 containers was calibrated using a U-8 volume source of ^{137}Cs (24FY039, Japan Chemical Analysis Center). Each sample was measured for 10,800 s. Radioactivity of the litter and soil samples was expressed as Bq/g dry weight (Bq/g dw), and that of earthworms as Bq/g fresh weight (Bq/g fw).

3.3 Results

3.3.1 Ambient dose equivalent rates at the sampling site

The median ambient dose equivalent rates showed a significant decrease from 2.15 μSv/h, to 1.67 μSv/h, to 1.35 μSv/h, in 2014, 2015, and 2016, respectively (Kruskal–Wallis test, $p < 0.001$; Fig. 3-3). Multiple comparisons by Scheffe's method indicated that the values continuously decreased from 2014 to 2016 ($p < 0.05$). The reduction rate of the ambient dose equivalent rate from 2014 to 2016 was 36.9%. The reduction rate was almost the same as that measured at the arthropod sampling site (35.5%), but the ambient dose equivalent rates at the earthworm site were higher than that for the arthropod site (Table 3-1). The decline in the ambient dose equivalent rates estimated by the physical decay of ^{134}Cs and ^{137}Cs is plotted as a dotted line in Fig. 3-3. The values determined by physical decay decreased to 1.77 μSv/h and 1.55 μSv/h in 2015 and 2016, respectively; these values are slightly higher than the actual ambient dose equivalent rates at the sampling site (Table 3-2).

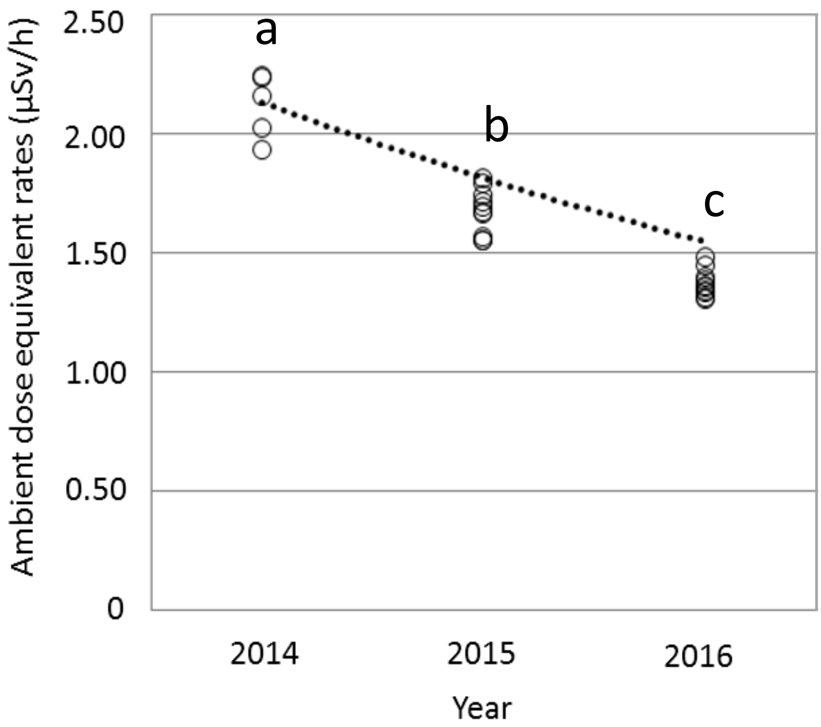

Fig. 3-3 Ambient dose equivalent rates at 1m above ground at the sampling site, significantly decreased from 2014 to 2016 (Kruskal–Wallis test, $p < 0.001$). In the graph, the letters above the plotted points denote significant differences from multiple comparisons determined by Scheffe's method ($p < 0.05$). The broken line represents the decline in ambient dose equivalent rates in 2014 based on physical decay of radiocesium.

Table 3-1 Ambient dose equivalents at each sampling site from 2014 to 2016.

µSv/h	2014	2015	2016
Arthropods sampling site	2.01	1.36	1.29
Earthworms sampling site	2.15	1.68	1.35

Table 3-2 Median values of measured ambient equivalent dose rates and estimated values due to physical decay of radiocesium.

µSv/h	2014	2015	2016
Measured value	2.15	1.68	1.35
Estimated value	2.15*	1.77	1.55

* The measured value is used at initial value to estimate ambient dose equivalent rates due to the physical decay of radiocesium.

3.3.2 Chronological changes in radiocesium concentration in earthworms

The concentration of ^{137}Cs in the litter was 44.9 Bq/g dw in 2014, which increased only slightly in 2015 (45.3 Bq/g dw), then dropped to 10.7 Bq/g dw in 2016. The concentrations of ^{137}Cs in the soil were 9.79 Bq/g dw, 7.14 Bq/g dw, and 18.0 Bq/g dw in 2014, 2015, and 2016, respectively (Table 3-3). In contrast, the median value of ^{137}Cs in earthworms from 2014 to 2016 did not change significantly; the values for 2014, 2015, and 2016 were 4.87 Bq/g fw, 5.30 Bq/g fw, and 4.67 Bq/g fw, respectively (Kruskal–Wallis test, $p = 0.878$; Fig. 3-4).

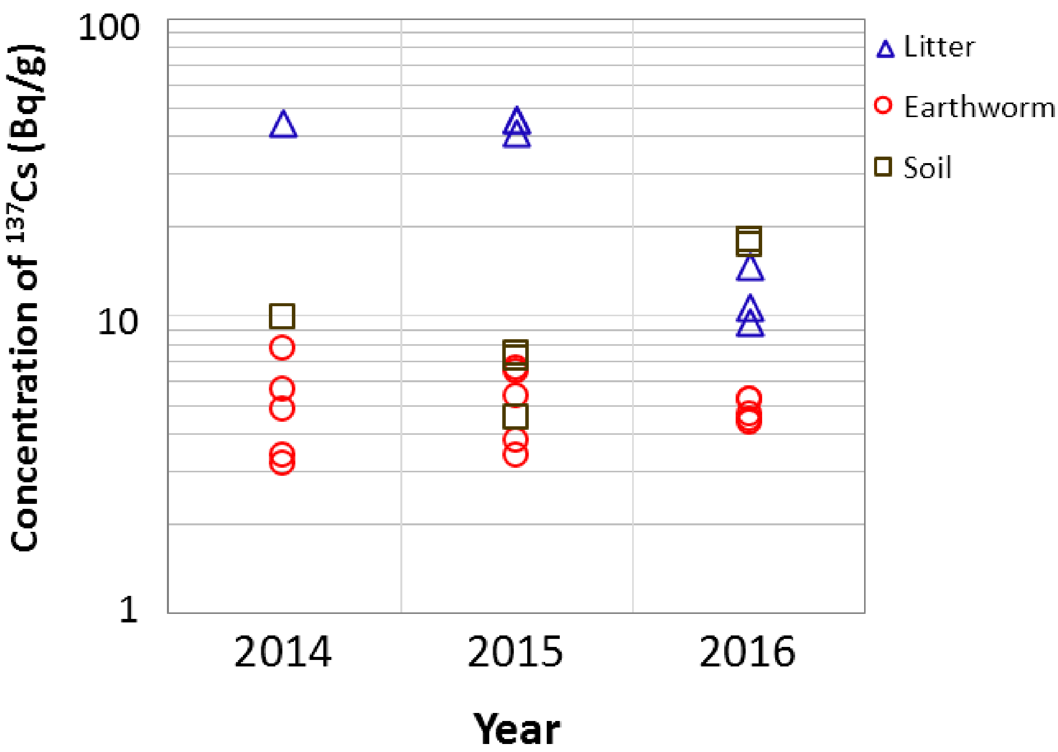

Fig. 3-4 Changes in the concentration of ^{137}Cs in the litter, earthworms, and soil from 2014 to 2016. Triangles, circles and squares represent the litter, earthworms and soil respectively. The concentration of ^{137}Cs in the litter and soil were determined from the dry weight, and that of earthworms was determined from the fresh weight. The concentration of ^{137}Cs in earthworms did not vary significantly over time after the accident from 2014 to 2016 (Kruskal–Wallis test, $p = 0.878$; multiple comparisons using Scheffe's method, $p < 0.05$).

Table 3-3 Concentrations of ^{137}Cs in samples from 2014 to 2016.

Year	Concentrations of ^{137}Cs (Bq/g)					
	Litter		Soil		Earthworm	
	n	Median (range)	n	Median (range)	n	Median (range)
2014	1	44.9	1	9.79	5	4.87 (3.22-7.77)
2015	3	45.3 (40.9-45.5)	3	7.14 (4.52-7.48)	5	5.30 (3.39-6.60)
2016	3	10.7 (9.52-14.6)	3	18.0 (17.0-18.0)	5	4.67 (4.39-5.28)

The concentration of ^{137}Cs in litter and soil were obtained as dry weight; the values for the earthworms were obtained as fresh weight. Earthworm samples numbers (n) indicate that 1 sample contains 1 individual in 2014 and 5 individuals in 2015 and 2016.

3.3.3 Comparison of radiosesium concentration in different feeding habits

Radiocesium concentration in grasshoppers, field crickets, Jorô spider and earthworms was compared in 2014. The median of ^{137}Cs concentration in earthworms was 4.87 Bq/g fw, which was about 85 times higher than that of grasshoppers, and over 30 times higher than that of Jorô spiders, which showed the highest level of ^{137}Cs among the 3 arthropod species examined (Fig. 3-5).

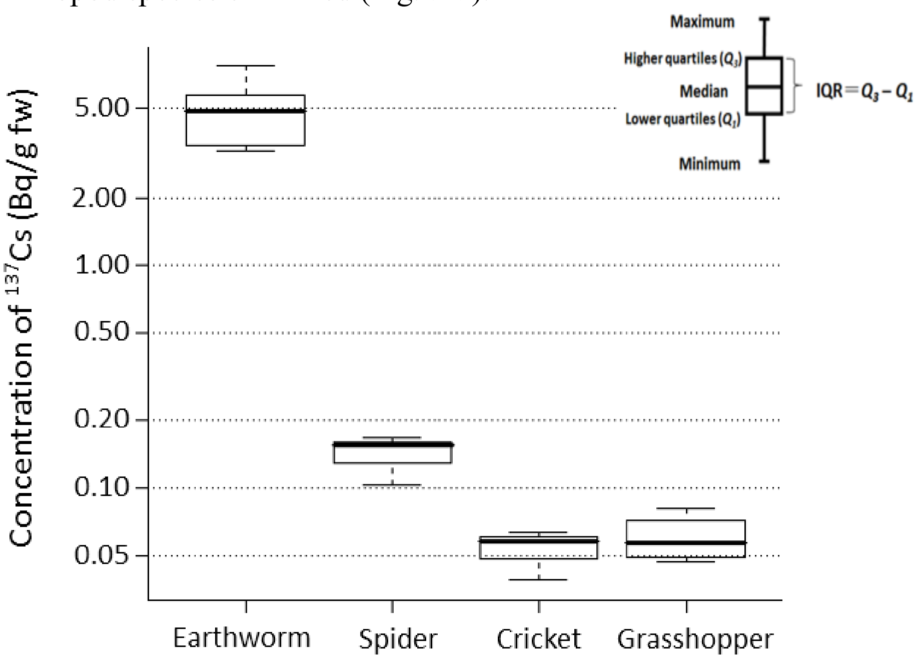

Fig. 3-5 Comparison of radioceium concentration in different feeding habits in 2014.

3.4 Discussion

3.4.1 Chronological changes in the ambient dose equivalent rates

The ambient dose equivalent rates significantly and continuously decreased from 2014 to 2016. The measured doses in 2015 and 2016 were slightly lower than the estimated values in which only the physical decay of radiocesium is considered. This suggests that the weathering (downward migration and/or runoff) of radiocesium affected the ambient dose equivalent rates, but was not as large at the sampling site. The ambient dose equivalent rates at the earthworm sampling site on the forest side were higher than those at the arthropod sampling site in the grassland and agriculture zone, as shown in Table 3-1. This finding coincides well with previous studies that report extremely slow downward migration and low-runoff of radiocesium from the floor of deciduous forests in Fukushima after the accident (Nakanishi et al., 2014; Niizato et al., 2016). Kinase et al. (2014) estimated that the ecological half-life of radiocesium is much longer in deciduous forests than in other land areas. It is possible that the temporal changes in ambient dose equivalent rates found in this study can be mainly attributed to the physical decay of radionuclides, although the precise mechanisms are not readily apparent from this study. These results also suggest that the radiocesium was retained in the forest floor during the survey period.

3.4.2 Chronological changes in the concentration of radiocesium in earthworms

As shown in Fig. 3-4, the soil concentration of ^{137}Cs increased from 2014 to 2016; in contrast, the concentration in the litter showed a decreasing trend during this period. The reason for these findings is readily apparent from the present study. A previous study of deciduous forests in Fukushima reported the rapid downward migration of radiocesium from the litter layer to the topsoil (Fujii et al., 2014). A similar finding was also reported for the period from 2013-2015, with large seasonal variations due to decomposition and input from contaminated litter fall (Takada et al., 2017). Therefore, the observed changes in the ^{137}Cs concentration in the litter and soil might represent the movement of ^{137}Cs on the forest floor due to decomposition and migration from litter to the topsoil.

The radiocesium concentration in earthworms did not significantly change from 2014 to 2016. It is well known that the feeding and egestion activities of earthworms homogenize the radiocesium on the forest floor (Tyler et al., 2001; Jarvis et al., 2010). This role of earthworms as bioturbators could partly explain why the ^{137}Cs concentrations in earthworms did not change much over the study period. The ^{137}Cs concentrations in detritivorous earthworms were maintained at the same level during the sampling period because they eat both highly contaminated litter and soil. This finding also demonstrates the importance of radiation protection for the environment and that the radiocesium concentrations in earthworms may be good indicators of the average contamination levels of the organic layer and surface of the forest, which are unevenly distributed (Koarashi et al., 2014).

The feeding habits of earthworms could provide another explanation for the lack of yearly change in the ^{137}Cs concentration in their bodies. Radiocesium is maintained in the organic horizon of forest soils by biological processes such as microbial immobilization and recycling (Brückmann and Wolters, 1994), and the long-term retention of radionuclides in these layers has frequently been attributed to microbiological activity (Steiner et al., 2002). Soil microorganisms are major food sources for earthworms, and protozoa and fungi are assumed to contribute a substantial portion to this diet (Edwards and Fletcher, 1988; Brown, 1995; Bonkowski and Sxhaefer, 1997). Moreover, earthworms have been reported to selectively feed on microorganisms (Doube et al., 1997; Bonkowski et al., 2000; Neilson and Boag, 2003). Epigeic earthworms in family Megascolecidae feed more on organic materials than earthworms of other ecological group (anecic and endogeic) (Uchida et al., 2004). Therefore, the earthworms collected in this study were consumers of soil microorganisms, which could explain, in part, why the radiocesium concentrations in their bodies did not show much change. It is worth noting that the zoological and ecological characteristics of earthworms may make them good indicators of the level of radiocesium contamination in the surface organic layers of forests.

3.4.3 Comparison of radiosesium concentration in different feeding habits

Comparison of radiosesium concentration in different feeding habits clearly shows that detritivores of earthworms are highest contaminated than other feeding habits. The concentration of earthworms was over 30 times higher than that of Jorô spiders which is highest concentration in the three arthropods.

Earthworms accumulate heavy metals such as cadmium (Cd), cooper (Cu), lead (Pb) and zinc (Zn) in their bodies when exposed to contaminated soils (Oste et al., 2001; Hobbelen et al., 2006; Li et al., 2010). This process is called bioaccumulation. The reason why the radiocesium in earthworm remains higher levels and whether earthworms can accumulate radiocesium or are not known, and an investigation is necessary. To clarify the mechanisms involved in this high concentration of radiocesium in earthworms, understanding for metabolism of radiocesium in earthworms is required.

4. Distribution of radiocesium in the earthworm body and the biological half-life of ^{137}Cs

4.1 Background and objectives of the study

Earthworms collected in Fukushima after the FDNPP accident showed higher concentrations of radiocesium than arthropods as was described in the previous chapter. The higher concentrations were maintained over three years from 2014 to 2016. To clarify the mechanisms contributing to this high concentration of radiocesium in earthworms, it is necessary to understand their metabolism of radiocesium.

Previous chapter discussed a possibility of bioaccumulation of radiocesium in the earthworm. Bioaccumulation data from earthworms have been reported for purposes of risk assessment in animals that feed on these invertebrates (Romijn et al., 1991; Heikens et al., 2001). Earthworms can transfer contaminants to species at higher trophic levels through the food chain. If earthworms accumulate radiocesium, there will be a substantial radiation risk to animals feeding on these invertebrates. Moreover, if radiocesium concentrated in specific organs of the earthworms, the radiation risk to the earthworms themselves will also increase. The habitat of the earthworms in Fukushima was highly contaminated and they ingested both soil and litter that were contaminated with radiocesium after the accident. Therefore, it is possible that some of the radiocesium ingested by the earthworms may accumulate in their bodies and, as a result, the concentration of radiocesium in the earthworms would be maintained at higher levels throughout the investigation period.

The biokinetics of radiocesium in earthworms has been previously reported, however, these experiments were conducted mainly focused on the family Lumbricidae, such as *Lumbricus terrestris* which is dominant in Europe (Brown and Bell, 1995; Sheppard et al., 1997). Among the three types of ecological subgroups of earthworms, *Lumbricus terrestris* is “anecic” which means it inhabits the middle layer of soil (Bouché, 1977; Lee, 1985). In contrast, the ecological subgroup of Megascolecidae evaluated in the present study is “epigeic” which inhabits the most surface layers among all the groups. The “epigeic” group is thought to be the most important for understanding both the behavior and radiation effects of radiocesium through the environment because most of the radiocesium accumulates in their litter and soil surface habitats. However, there have been no studies on the metabolism of radiocesium in the epigeic earthworm family Megascolecidae, even though the distribution of earthworm families in Japan is dominated by Megascolecidae, comprising 95% (Ishizuka, 2015). Therefore, it is necessary to conduct experimental studies on the biokinetics of radiocesium in the family Megascolecidae.

The objectives of this chapter are to clarify the biokinetics of radiocesium in the Megascolecidae earthworm family and discuss why radiocesium concentrations in earthworms were maintained at higher levels over three years. In addition, we investigated whether radiocesium accumulates in specific organs of the earthworms or showes other distribution patterns.

To evaluate this, the distribution of radiocesium in the bodies of the earthworms was visualized by autoradiography and the radiocesium concentrations in their body wall muscle, gut, and other organs were determined. In parallel, a clearance experiment was conducted to estimate the biological half-life of radiocesium in the earthworms.

4.2 Materials and methods

4.2.1 Autoradiography

Autoradiography was performed using high-resolution imaging plates (BAS-IP MS 2025E, Fujifilm, Co., Japan.) exposed for 8 day at −80°C after contact with the plate. The plate was read with a scanner (Typhoon FLA7000, GE healthcare, Japan Co.) to take autoradiographic images. The autoradiography was conducted on earthworms collected in 2014 and 2015.

4.2.2 Sample preparation and measurement of ^{137}Cs in earthworms

To measure the ^{137}Cs accumulation in each region of the body, 25 earthworms were dissected and the intestines, body wall muscles, and other organs were separated. An additional 75 earthworms were collected in 2016 for the clearance experiments.

The activity concentration of ^{137}Cs was measured using the same methods as described in 3.2.3 to determine the concentration in each body part of the earthworm using a U8 container for the measurements of individual earthworms were used plastic petri dishes (60mm in diameter, 15mm high).

The counting efficiency of samples in the petri dish was calibrated using the KCl method, which used an efficiency curve normalized to the gamma-ray peak for 1460 keV from ^{40}K in KCl placed in the same type of vessel (Fujiwara et al., 2015). Each sample was measured for 10,800–27,000 s.

4.2.3 Estimation of the biological half-life of ^{137}Cs in earthworms

The biological half-life of ^{137}Cs was estimated in the earthworms collected in 2016. The earthworms were transported to the laboratory with soil and litter from the sampling site. They were moved from the contaminated sampling site medium to a non-radioactive medium for determining the whole-body clearance of ^{137}Cs. The ^{137}Cs radioactivity of five individuals was measured at 1, 3, 6, 12, 24, 48, 120, 240 and 360 h after the moving. The concentration of ^{137}Cs at each time point was defined as the median value of five earthworms. To estimate the biological half-life (T_b) of ^{137}Cs in these earthworms, the following double exponential equation was applied (Eq. (1)):

$$A_t = A_{0_f} e^{-\lambda_f t} + A_{0_s} e^{-\lambda_s t} \qquad (1)$$

where A_t is the concentration of ^{137}Cs (Bq/g) at time t, A_0 is the initial concentration of ^{137}Cs (Bq/g) (t = 0), and λ_f and λ_s are the elimination rate constants for the fast and slow clearance, which was caused by simple passage through the intestine and physiological clearance of assimilated ^{137}Cs, respectively. Log-transformed data were used to estimate A_0 and λ using the non-linear least squares fitting method.

4.3 Results

4.3.1 Autoradiographs of earthworms

Fig. 4-1 shows an autoradiograph of an earthworm with that of soil in a plastic bag. The distribution in the earthworm did not appear to be uniform, and the radiocesium was concentrated mainly in the digestive tract along the midline of its body. Compared to the autoradiograph of dry soil, the level of radioactivity in the earthworm was similar to the soil. It was difficult from this autoradiograph to determine where and how the radiocesium was distributed in the organs of the earthworm. Thus, the other worms were dissected then exposed to the imaging plate. Fig. 4-2 shows an autoradiograph taken after the dissection. The concentration of radiocesium in the body wall muscle was very low and could not be detected by the imaging plate. There were no specific regions or points where the radiocesium was accumulated. In contrast, the concentration in the intestine was much higher and showed a non-uniform distribution. Microscopic observations showed that the parts of the intestine with higher radiocesium activity as determined by autoradiography corresponded to the gut contents (feces) in the intestine. The other organs, including the reproductive organs, were dissected from the body wall muscle while still attached to the anterior portion of intestine. Autoradiography showed no specific or remarkable deposition of radiocesium in these organs.

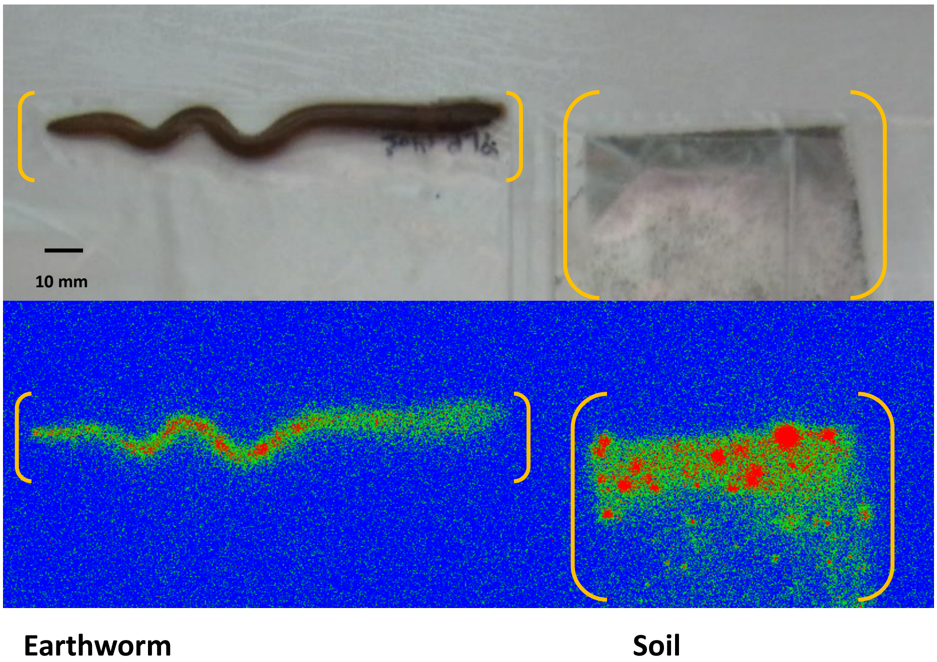

Fig. 4-1 Autoradiographs (bottom) and photographs (top) of an earthworm and habitat soil. The earthworm was exposed in fresh condition, and the soil (≤5 cm) was in a dry condition when spread on the plate. Red and green areas indicate high and low concentrations of radiocesium, respectively; blue areas indicate the background concentration.

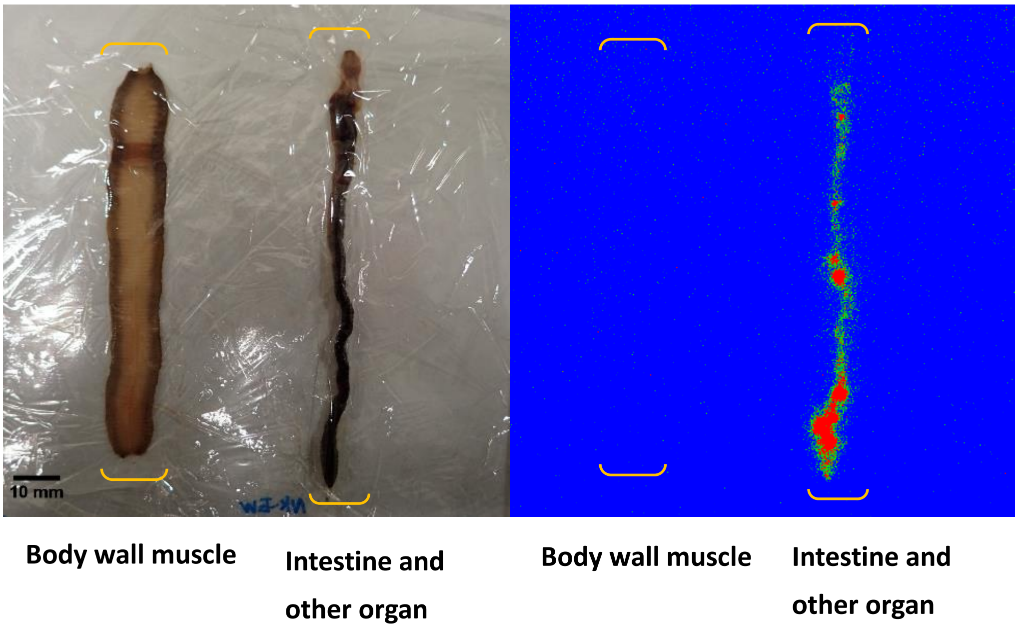

Fig. 4-2 Autoradiographs (right) and photographs (left) of a dissected earthworm. The earthworm was dissected into two parts, body wall muscle and intestine with other organs.

4.3.2 Concentrations of ^{137}Cs in different part of the earthworms

The concentrations of ^{137}Cs in the intestines, body wall muscles, and other organs in the earthworms were determined using a germanium semiconductor detector. The median concentrations of ^{137}Cs in intestine, body wall muscle, and other organs were 6.48 Bq/g fw, 0.17 Bq/g fw, and 0.10 Bq/g fw, respectively (Fig. 4-3). The ratio of the ^{137}Cs concentration in the body wall muscles to that in the intestines was 0.02. The percentages of ^{137}Cs in the earthworm intestines, body wall muscles, and other organs were 95.9%, 2.6% and 1.5%, respectively, of the total retained ^{137}Cs.

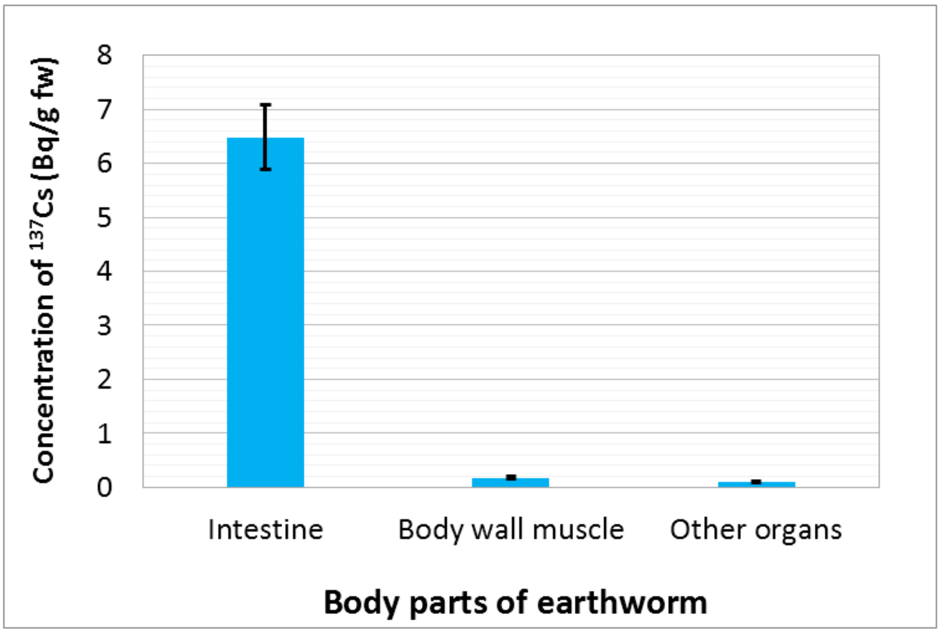

Fig. 4-3 Concentrations of ^{137}Cs in each part of dissected earthworms. The error bars indicate standard deviations.

4.3.3 Clearance of ^{137}Cs and its biological half-life

As shown in Fig. 4-4, the clearance curve of ^{137}Cs from the earthworm body seemed to be bi-phasic (i.e., had a two-component clearance). By fitting the curve to a double exponential equation (Eq. (1)), the half-life of the first phase (T_b fast) was calculated as 0.10 days. The second phase of clearance was much slower with a half-life (T_b slow) of

27.4 days. The fast and slow phases were estimated to have cleared 95.6% and 4.4%, respectively, of the total retained ^{137}Cs (Table 4-1).

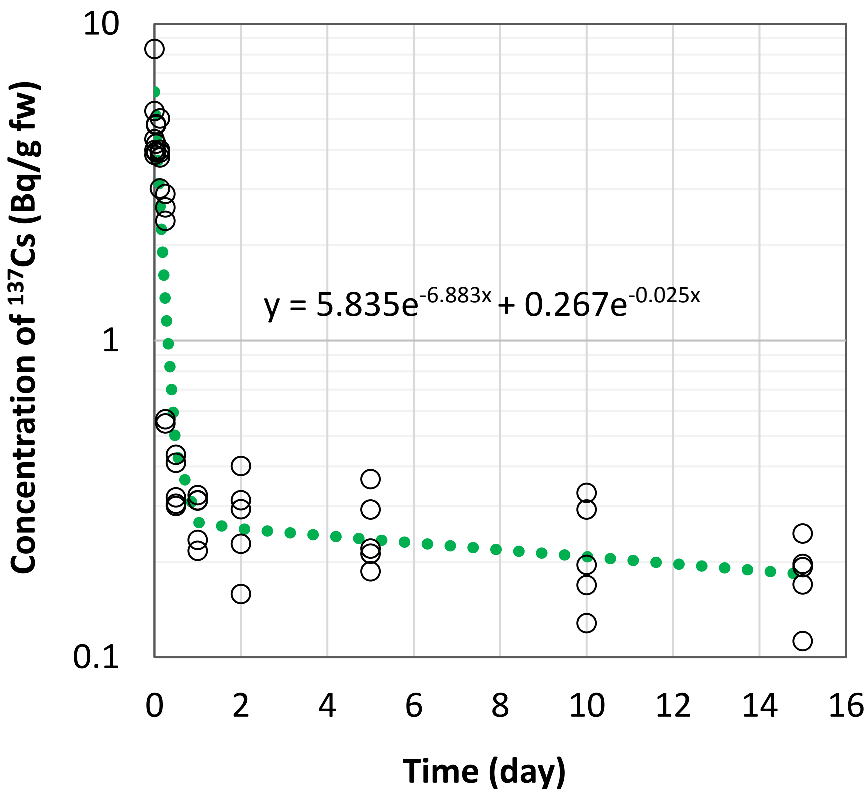

Fig. 4-4 Clearance of ^{137}Cs from the earthworm body. The clearance curve appeared to be bi-phasic. Approximately 95.6% was cleared with a half-life of 0.1 days, and the remaining 4.4% was cleared with a half-life of 27.4 days.

Table 4-1. Model components of the biological half-life of ^{137}Cs

Component	Model	Double exponential				
	Equation	$y = A_f e^{-t_1 x} + A_s e^{-t_2 x}$				
			SE	*t*-value	*p*-value	Ratio (%)
$T_{b(fast)}$	A_f	5.835	0.727	8.031	< 0.001	95.6
	t_1	6.883	0.786	8.740	< 0.001	
$T_{b(slow)}$	A_s	0.267	0.033	8.004	< 0.001	4.38
	t_2	0.025	0.015	1.716	0.093	

SE: Standard error

4.4 Discussion

The autoradiograph of an earthworm body showed that the radiocesium was distributed mainly in its intestines with little found in the other tissues of the body (Figs. 4-1, 4-2). Given the limitations of these experiments, it was difficult to determine the exact regions showing higher concentrations of radiocesium in the intestine. However, the regions showing higher levels corresponded to the bulk contents (feces) of the intestine, suggesting that the observed radioactivity was mainly attributabed to the contents and not to the intestinal wall. Quantitative measurements obtained with a germanium detector showed that 95% of the ^{137}Cs was located in the intestines (Fig. 4-3). Therefore, it can be concluded that most of the radiocesium ingested by earthworms is excreted rapidly through the digestive tract without absorption into the intestinal wall.

Approximately 95.6% of the total radioactivity was cleared during the initial rapid phase, while 4.4% of the ^{137}Cs was cleared in the second slower phase. These values correspond with the abundance ratio of ^{137}Cs in the earthworms, the majority of which was in the intestine and the rest of which (4.0%) represented the values of the body wall muscle and other organs combined. Previous studies on the biological half-life of radiocesium in earthworms are summarized in Table 4-2; in this study, the T_b fast value (0.10 d) was a little faster than reported in the other three studies, and the T_b slow (27.4 d) was within the range found by Brown and Bell (1995). Therefore, these results demonstrate that there is little difference in radiocesium metabolism between earthworms of the families Megascolecidae and Lumbricidae.

The present study on the abundance ratio of ^{137}Cs in different parts of the earthworm and the biological half-life indicate that ^{137}Cs will not be highly bioaccumulated in earthworms. Hasegawa et al. (2015) previously investigated the changes in radiocesium bioavailability in epigeic earthworms after the nuclear accident and reported a decrease in the initial phase from 2011 to 2013. Radiocesium is strongly fixed to soil minerals in a time-dependent manner; therefore, the body wall muscle of earthworms will not show long-term bioaccumulation of radiocesium.

The present study shows that radiocesium did not accumulate in the bodies of earthworms nor in specific organs or other body parts. Thus, the concentration of radiocesium in earthworms will not be higher than levels in the environmental medium. This is critical information for radiation dose estimations of earthworms living in the contaminated area. A large proportion of radiocesium shows long-term accumulation in the soil surface layer in forests. The radiocesium concentrations in the gut contents of the earthworms is dependent on the contamination levels in their habitat media, that is, the radiocesium concentrations of earthworms will be maintained at a higher level for long-term. This suggests that detritivore species occupying the same habitat as earthworms are also high, and become a primary transfer pathway for radiocesium through the food web. Moreover, given the ecological characteristics of earthworms, they are expected to show the highest radiation exposure among most species in the environment. This means that accurate dose assessment in earthworms may be one of good indicators of contamination for environmental radiation protection.

Table 4-2 Comparison of the biological half-life of radiocesium (^{134}Cs and/or^{137}Cs) in this study and previous studies.

Family	Genus	Ecological type	Media	Biological half-life (day)		References
				T_b fast	T_b slow	
Lumbricidae	*Lumbricus terrestris*	Anecic	Litter (Apple leaves)	0.16-0.33	25-54	Brown and Bell, 1995
Lumbricidae	*Lumbricus terrestris*	Anecic	Soil	0.20-0.27	15-26	Brown and Bell, 1995
Lumbricidae	*Lumbricus terrestris*	Anecic	Litter	1.4	24	Sheppard et al., 1997
Megascolecidae	Unknown	Epigeic	Litter and soil	0.10 ± 0.01	27.4 ± 16.0	This study

±: Standard error.

5. Radiation doses of the earthworms and spiders and related risk assessments

5.1 Background and objectives of the study

As described in the previous chapter, earthworms have been continuously contaminated with radiocesium after the FDNPP accident. Although radiocesium did not accumulate in specific organs of the earthworms, the concentration of radiocesium in the organisms was of a comparable level to that of their habit (litter and surface soil). The surface organic horizon is a major source and cause of retention of radiocesium in the forest ecosystem (Kruyts and Delvaux, 2002; Steiner et al., 2002). In the long term, epigeic earthworms spend their time eating and crawling in the highly contaminated organic surface layer. Therefore, these earthworms are subject to both internal and external radiation exposure throughout their whole lifetime. Their exposure is further increased owing to the passage of contaminated organic matter through their digestive tracts, and they also lack the chitinous exoskeleton of other invertebrates such as arthropods. These factors suggest that epigeic earthworms are one of the groups in the ecosystem with the highest radiation exposure. Because of their ecological characteristics and importance to the ecosystem, these earthworms were selected to be one of the reference animals and plants (RAPs) that are evaluated in relation to environmental radiation protection (ICRP, 2008).

Of the three types of arthropod investigated in the present study, the Jorô spider showed the highest concentration of radiocesium. This concentration remained unchanged in the study period (2012–2016), suggesting that the spiders received constant and relatively high radiation exposure from the internal radiocesium. Therefore, it is useful to evaluate the Jorô spider as a model arthropod for the study of radiation dose, particularly as these spiders may have received high internal radiation doses as a result of the FDNPP accident.

The basic quantity used in determining radiation exposure is the absorbed dose, which is defined as the amount of energy absorbed per unit mass of tissue contained in an organ or organism. The absorbed dose is given in units of Gray (Gy). The biological effects of radiation are subject to wide variations, depending on the dose per unit time (absorbed dose rate, Gy/h) even in cases where different organisms are exposed to the same dose (absorbed dose, Gy). The biological effects of radiation increase with exposure at a high dose rate rather than that at a low dose rate. To clarify the correlation between radiation exposure and radiation effects on earthworms, an accurate assessment of absorbed dose is necessary. Studies on the effects of radiation on non-human biota in Fukushima were conducted after the FDNPP accident (Hiyama et al., 2012; Møller et al., 2013; Akimoto, 2014; Ochiai et al., 2014), although accurate dose assessments on wild species are limited (Kubota et al., 2015; Fuma et al., 2015).

A field study was conducted after the Chernobyl accident to ascertain the effects of radiation on earthworms. Soil invertebrates exhibited higher absorbed dose rates than other animals because their habitats were highly contaminated. The population densities and species diversities of soil invertebrates were decreased in Chernobyl with an absorbed dose above 30 Gy; the population densities of earthworms in particular decreased owing to their high radio-sensitivity during the egg and juvenile life stages (Krivolutzkii et al., 1992). The effects of the Chernobyl accident on arthropods were observed in terms of a decrease in species diversity on the soil mesofauna. Only 15 species of oribatid mite were found near the Chernobyl NPP, compared to 25 species on the edge of the 30 km zone and 33 species on a control plot 70 km from the plant (Krivolutzkii and Pokarzhevskii, 1992).

A laboratory study of the radiation effects on earthworms reported that the $LD_{50/30}$ (Lethal dose of 50% within 30 days) of gamma rays for *Lumbricus terrestris* was 680 Gy (Haffner et al., 1973; Reichle et al., 1972), while this was 650 Gy for *Eisenia foetida* (Suzuki and Egami, 1983). Young earthworms (*E. foetida*) showed completely inhibited growth when subjected to 100 Gy gamma irradiation, while gamma irradiation in the range 10–20 Gy led to decreased proliferation of the epidermal cells (Suzuki and Egami, 1983). Chronic gamma irradiation effects on intergeneration indicated no significant effects on the growth of F0 adults for absorbed gamma dose rates up to 1 Gy/day. The growth of the F1 juveniles was not inhibited up to dose rates of 264 mGy/day, while the dose rates caused some exterior abnormalities (Hertel-Aas et al., 2007).

The effects of acute irradiation on arthropods are summarized in the International Database on Insect Disinfestation and Sterilization (IDIDAS) (IAEA/IDIDAS, 2018) for its use in pest control applications such as the sterile insect technique (SIT) (Hendrichs, 2000; Vreysen, 2001). These data were collected for the purpose of pest control and for their economic importance in relation to agricultural production and food safety. Thus, only three spider species were noted in a database of more than 2750 references. These data focused on the effects of high dose rate irradiation on the reproductive success of arthropods. In the case of the web spider *Argiope keyserlingi*, which is of the same family as the Jorô spider, the dose required for 100% male sterility was 40 Gy. The doses required for 100% sterility of the *Holocnemus pluchei* and *Stegodyphus lineatus* spider species were 20 Gy and 150 Gy, respectively (IAEA/IDIDAS, 2018). Data on correlations between the dose rates and radiation effects in the arachnid order were not found. Thus, these data were replaced by that of bees, which were the only insects in the RAPs. The capacity of the wasp population (*Dahlbominus fuscipennis*) to reach the third generation failed at dose rates of 2.4 Gy/day. At 1.2 Gy/day, after two generations, the population was reduced to less than 20% of the control population but did then survive for seven generations (Riordan, 1964). At 1.15 Gy/day, the number of disintegrating oocytes in females decreased and a decline in the number of offspring was observed (Baldwin, 1968). The aims of this chapter are to estimate the absorbed dose rates in the Jorô spider and Megascolecidae earthworm in the study site and discuss the radiation risks of these species after the FDNPP accident.

5.2 Materials and methods

5.2.1 ERICA assessment tool

The ERICA (Environmental Risk from Ionizing Contaminants: Assessment and management) assessment tool is a software based on the ERICA integrated approach used to assess radiation effects on non-human biota (Brown et al., 2008). The tool has been employed in radiation risk assessment for wild species in Fukushima after the FDNPP accident (Kubota et al., 2015; Fuma et al., 2015; Garnier-Laplace et al., 2011; Kryshev et al., 2012; Fisher et al., 2013; Strand et al., 2014). The ERICA approach is based on the assessment of reference animals and plants (RAPs), for which basic biological characteristics of particular types of 12 animals and plants are assumed to assess the effects of radiation on the ecosystem. The earthworm was selected to be one of the RAPs; thus, absorbed dose rates can be calculated using this tool. The dose-rate models are based on Monte Carlo techniques that simulate radiation transport. The models are constructed with the assumption that the dosimetry of an organism may be represented by ellipsoids, with a homogeneous radiation distribution in the organisms.

The assessments are conducted in three tiers: Tier 1 assessments are based on media concentration and pre-calculated environmental media concentration limits in order to estimate risk quotients; Tier 2 calculates dose rates and allows the editing of several parameters including concentration ratios, distribution coefficients, percentage of dry weight soil or sediment, dose conversion coefficients, radiation weighting factors, and occupancy factors; Tier 3 provides the same flexibility as Tier 2 and allows the option to run the assessment probabilistically, if the underling parameter distribution functions are defined. The dose rate calculations in this study were conducted using Tier 2.

5.2.2 Absorbed dose rate calculations

The absorbed dose rates of the earthworms were calculated using the ERICA assessment tool 1.2. The absorbed dose rates of the Jorô spider were calculated with the ERICA tool in the case of the internal dose rates, while using the ambient equivalent dose rates for the external dose rates. As the earthworm is included in RAPs, the appropriate exposure settings may be used in the ERICA tool in terms of both internal and external dose rate. In contrast, the web spider is not included in RAPs; thus, the ERICA tool setting for external dose rate is not suitable for these calculations. Therefore, the methods of dose rate calculation differed between the two species. The web-making Jorô spider spends its time on a web in the air, and thus, the ambient equivalent dose rate provides a suitable external dose rate for the spider.

Tier 2 was selected in the ERICA tool and the ^{134}Cs and ^{137}Cs isotopes were chosen. The geometry of the earthworm was modified to coincide with that of the epigeic earthworm; a height of 0.005 m, width of 0.005 m, and length of 0.06 m. The organism mass was set to 0.001076 kg, which is the average mass of the earthworms used in the study. For the Jorô spider, the following geometry was applied: a height of 0.0008 m, width of 0.0008 m, and length of 0.0025 m. The organism mass was set to 0.000415 kg, which is the average mass of the earthworms collected.

An occupancy factor, the fraction of time a given organism spends at a location in its given habitat, of 1.0 was used, together with the “In-soil” setting for the earthworms, because epigeic earthworms usually remain in the soil or litter. Radiation weight factors of 1.0 were selected for β/γ-rays and 3.0 for low-energy β-rays, which are the default values. To perform conservative assessments, the highest median radiocesium concentration of the earthworms through the three-year investigation was used for the calculations. The following equation was used to calculate absorbed dose rates:

$$D_{i.ad} = D_{i,ad}^{int} + D_{i,ad}^{ext} \quad (2)$$

Here, $D_{i.ad}$ is the absorbed dose rate of the earthworm from radionuclide i, $D_{i,ad}^{int}$ is internal dose rate to the earthworm from radionuclide i in its own body, and $D_{i,ad}^{ext}$ is the external dose rate to the earthworm from radionuclide i in litter.

5.2.3 Radiation risk assessments on earthworms and spiders

A reasonable amount of data describing various types of radiation effects on organisms is present in the literature. However, almost all of the data are related to high dose rates and total doses; studies related to low dose rates are limited. Therefore, it is difficult to make assessments or judgments concerning lower dose rates related to long-term exposure in the environment.

The ICRP presents a pragmatic approach to assessing the effects of radiation at low dose rates using derived consideration reference levels (DCRLs). These are bands of dose rates in which certain effects have been reported or might be expected, made using information from the database (ICRP, 2008). Thus, the calculated absorbed dose rates of the earthworms and spiders were referred to the DCRL of the earthworm to assess radiation risk.

5.3 Results

5.3.1 Absorbed dose rates of earthworms and spiders

The absorbed dose rates of earthworms that were calculated using the ERICA assessment tool are summarized in Table 5-1. The absorbed dose rate of $^{134+137}Cs$ was 23.8 µGy/h for external exposure and 0.88 µGy/h for internal exposure, and the total was 24.5 µGy/h. The external absorbed dose rate was dominant in the case of the earthworm and the ratio of internal/external dose rate was 0.04. The absorbed dose rate of radiocesium for the earthworm was 96% for the external exposure. The absorbed dose rates of the Jorô-spider are presented in Table 5-2, using the average ambient radiation dose rates at the sampling sites. The absorbed dose rates for internal exposure were estimated by the ERICA tool to be 0.2 µGy/h. The absorbed doses for external exposure are assumed to be the same as the ambient equivalent dose rate (for example, a median of

3.74 μSv/h for 2014). The total absorbed dose rate for the Jorô spider was 3.94 μGy/h, while the ratio of the internal/external dose rates was 0.05, at approximately 95% for the external absorbed dose rate. The Jorô spider may receive additional external radiation from the plants near their web, but for the sake of straightforward evaluation, the external radiation doses were assumed to be equal to the ambient equivalent dose, measured at 1 m above the ground.

Table 5-1 Activity concentrations for earthworm and litter and estimated absorbed dose rates

Radionuclide	Activity concentration		Absorbed dose rate μGy h^{-1}		
	Earthworm Bq kg^{-1} fw	Litter Bq kg^{-1} dw	External	Internal	Total
^{134}Cs	1770	12000	10.0	0.17	10.2
^{137}Cs	5310	45400	13.8	0.71	14.5
Total	7080	46600	23.8	0.88	24.7

Table 5-2 Activity concentrations for the Jorô spider, ambient dose equivalent rates, and estimated absorbed dose rates

Radionuclide	Activity concentration		Absorbed dose rate μGy h^{-1}		
	Jorô Spider Bq kg^{-1} fw	Ambient dose equivalent μGy h^{-1}	External*	Internal	Total
^{134}Cs	124	-	-	0.02	-
^{137}Cs	189	-	-	0.18	-
Total	313	3.74	3.74	0.20	3.94

* The Jorô spider may receive additional external radiation from plants near their web. Here, the external radiation doses were assumed to equal the ambient radiation equivalent dose measured at 1 m above the ground.

5.3.2 Radiation risk assessments on earthworms and spiders

The absorbed dose rate of earthworms at the sampling site was 0.59 mGy/day. The DCRL supplied an assessment of “effects unlikely” (referring to radiation effects) using the benchmark dose rates of reference earthworms in the range 10–100 mGy/day (Fig. 5-1) (ICRP, 2008). In the case of the Jorô spider, the absorbed radiation dose was calculated to be 0.09 mGy/day, which is much lower than the DCRL for insects (bee) in the range 10–100 mGy/day (Fig. 5-1). Therefore, if the DCRL of the ICRP are used as the criteria for risk assessment, it is unlikely that there were radiation effects caused by radiocesium exposure at the sampling site during the sampling period.

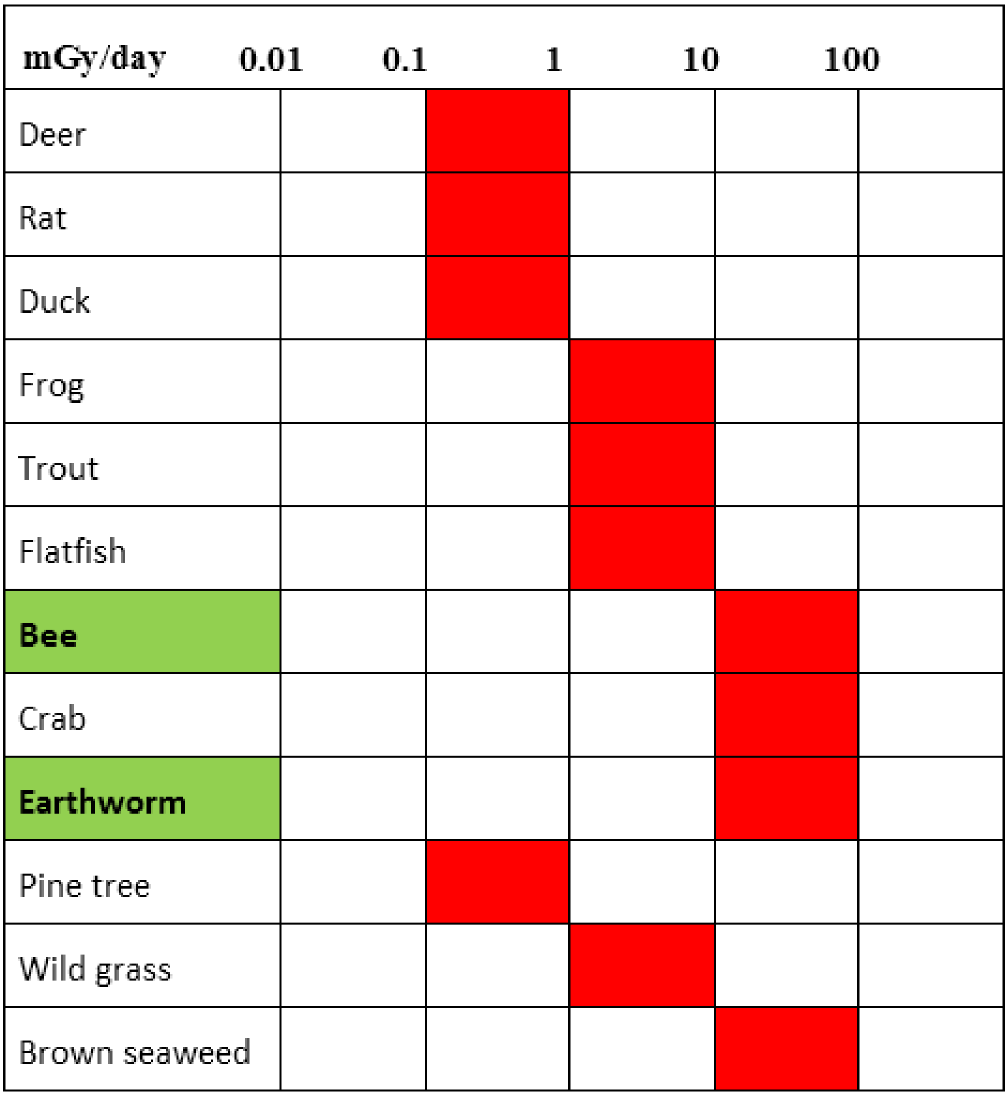

Fig. 5-1 Derived Consideration Reference Levels (mGy/day) for 12 Reference Animals and Plants (ICRP. 2008).

5.4 Discussion

The radiation dose rates of the earthworms and spiders were calculated using the ERICA assessment tool. Only the ^{134}Cs and ^{137}Cs radionuclides were used because the earthworm sampling has been conducted since 2014, and short-half-life radionuclides such as ^{131}I, ^{129m}Te, and ^{110m}Ag were not detected in the samples. The dose rate of the earthworms at the sampling site was calculated to be 0.59 mGy/day. This value was below the derived consideration reference levels for earthworms of 10–100 mGy/day (ICRP, 2008). The certain effects of radiation on juvenile earthworms have been observed at a lowest dose rate of 96 mGy/day (Suzuki and Egami, 1983). This means that the estimated dose rate of the earthworms at the sampling site was more than 160 times lower than the lowest value for certain radiation effects obtained in an earlier study. Therefore, there are no expected radiation exposure effects on the earthworms at the sampling site within the sampling period. However, it should be noted that the dose rates of the earthworms were calculated using only the gamma-emitting radionuclides of ^{134}Cs and ^{137}Cs, owing to the use of a sampling period from 2014. No short-half-life radionuclides such as ^{131}I, ^{129m}Te, and ^{110m}Ag were included in the study. It could be expected that the effects of radiation on earthworms would be more noticeable in the initial phase after the accident, including effects related to short-half-life radionuclides.

As shown in Table 5-2, the absorbed radiation doses for the Jorô spider were much lower than those of the earthworm. The concentration of radiocesium is higher at the leaves and the surfaces of tree trunks and the ambient dose rates were higher near the trees than at the measurement site (1 m above the ground in an open field). Therefore, the external radiation, to which the Jorô spider was exposed, may be slightly higher than the ambient radiation equivalent dose that was measured 1 m above the ground. However, this additional increase in the dose may not be sufficiently large to affect the risk assessment.

Short-half-life radionuclides such as ^{129m}Te and ^{129}Te (half-life: 33.6 d) contribute to the β-ray dose rate initial phase after deposition. In general, approximately 80% of the total absorbed dose for animals and plants after the Chernobyl accident was attributed to the first three months after the accident, with a 95% contribution from β-rays (UNSCEAR, 1996). β-rays are not directly related to external doses that concern humans as these are easily shielded by few millimeters of thick skin, but these could affect small organisms such as earthworms. In particular, the absorbed dose rate of β-rays is ten times that of γ-rays in the soil during the 20 days after deposition (Endo et al., 2014).

Endo et al. (2014) estimated cumulative 70 µm β-ray doses from ^{129m}Te, ^{129}Te, ^{131}I, ^{132}Te, ^{132}I, ^{134}Cs and ^{137}Cs with a deposition of 1000 kBq/m^2 for ^{137}Cs after the FDNPP accident, which assumed the presence of small organisms and human skin. The web-making Jorô spider lives above the ground, thus β-ray exposure is low. By contrast, the earthworm is exposed to β-rays through contaminated soil and litter, thus 70µm β-ray dose rates should be calculated.

The averaged 70 µm β-ray dose rate up to 30, 60, and 90 days after deposition of 1000 kBq/m^2 for ^{137}Cs were estimated by Endo et al. (2014) to be 2.0, 1.3, and 1.0 mGy/day in the soil, respectively (Endo et al., 2014). The initial deposition densities of ^{137}Cs at the sampling site reached 3000 kBq/m^2 (MEXT, 2011), thus the β-ray dose rate at the sampling site would be expected to reach a maximum three times higher than the above values. That is, β-ray dose rate at 30 days after the accident at the sampling site with maximum ^{137}Cs deposition densities (3000 kBq/m^2) was approximately 6.0 mGy/day in the soil. This value is still below the DCRL of the earthworm, at 10–100 mGy/day. Therefore, even when the contributions of short half-life radionuclides are taken into consideration, no effects of radiation on the earthworms would be expected at the sampling site.

It is necessary to estimate the β-ray dose rate at high deposition densities of ^{137}Cs near the plant. The highest deposition density of ^{137}Cs near the plant was 14700 kBq/m^2 (MEXT, 2011), thus the averaged β-ray dose rate up to 30, 60, and 90 days after the accident was approximately 29.9, 19.4, and 15.0 mGy/day in the soil (Table 5-3), respectively. The β-ray dose rate in the soil after 30-90 days was within the range of the DCRL of the earthworm. Therefore, the radiation risk of the earthworms should be considered in initial 90 days after the accident in the highest deposition area near the plants.

Table 5-3 70 µm dose rate for the highest deposition densities of ^{137}Cs after deposition

mGy/day	30 days	60 days	90 days
Ground surface	17.2	11.0	8.7
In soil	29.9	19.4	15.0

6. General discussion

6.1 Transfers of radiocesium to arthropods and earthworms through the food chain

In this study, radiocesium concentrations in arthropods and earthworms following the FDNPP accident were investigated. It was found that although concentrations in spiders and earthworms did not decrease significantly over time, they did decrease in grasshoppers and crickets. This pattern appears to be related to the trophic positions of these different group, as discussed in Chapters 2 and 3.

Behavior of radiocesium in forest ecosystems is well investigated in relation to the links between trees and soil or litter, whereby radiocesium in the soil is absorbed by trees and accumulates on the forest floor via litterfall, and is subsequently reabsorbed after organic material decomposition (Kato et al., 2012; Teramage et al., 2014; Loffredo et al., 2014). This suggests that radiocesium is circulated within the forest ecosystem (Yoshida et al., 2004). To date, however, there have been no quantitative reports on the contributions of invertebrates and microorganisms in these processes in forests or grasslands. This study is the first to demonstrate that radiocesium is transferred to organisms via the food chain, and that concentrations of this radionuclide do not decrease significantly in generalist spiders aftermath of contamination events. Moreover, since radiocesium transfer appears to differ according to the different feeding habits of organisms, it is likely that various trophic pathways are involve in its transfer.

Radiocesium concentrations in earthworms were found to be significantly higher than those in arthropods, with no appreciable decrease observed over time. There are at least two possible explanations for these observations, namely, bioaccumulation of radiocesium in earthworm body tissues, or regular intake via a highly contaminated diet. Autoradiography and whole-body retention experiments indicated that bioaccumulation is not probably responsible (Chapter 4). Moreover, the concentrations of radiocesium in leaf litter decreased over time after the FDNPP accident, whereas concentrations in soil below the litter layer increased. These findings thus suggest that the concentrations of radiocesium in earthworms are steadily maintained at high levels due to their ingestion of both litter and soil. In general, radiocesium migration from litter to soil occurs via weathering. Earthworms contribute to this process as bioturbators across both litter and soil layers, thereby increasing the vertical migration of radiocesium.

Figure 6-1 shows the overall trophic pathways of radiocesium, including its transport via grazing and detritus food chains in arthropods and earthworms. Given that earthworms might play an important role in the transfer of the radiocesium from litter to soil layers, further studies should be conducted to gain a more detailed understanding of the quantitative involvement, seasonal variation, and densities of these organisms with respect to the behavior of radiocesium in forest ecosystems.

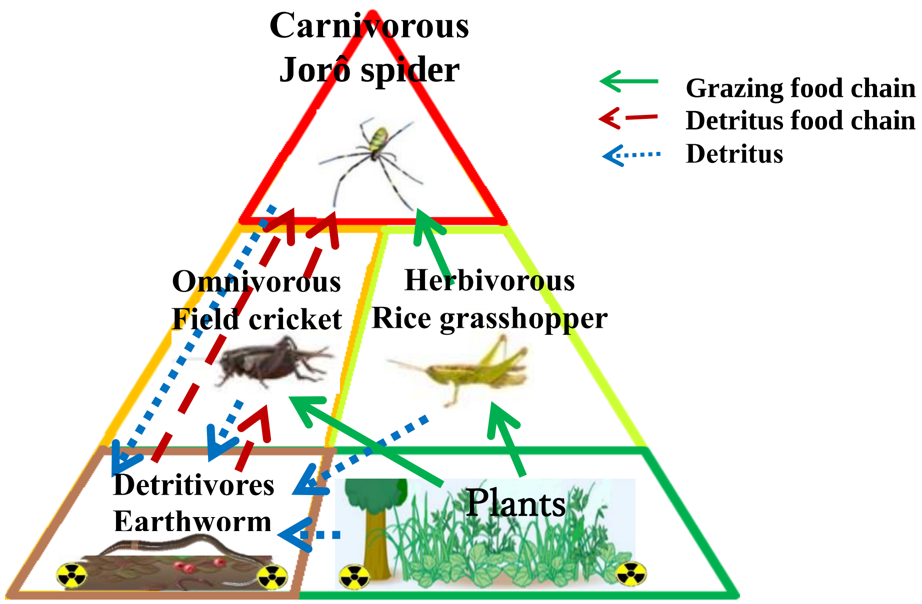

Fig. 6-1 Transfer pathways of radiocesium through the invertebrate food chain. Arthropods and earthworms represent carnivorous (jorô spider), omnivorous (field cricket), herbivorous (rice grasshopper), and detritivorous (earthworm) trophic habits.

6.2 Metabolism of radiocesium in earthworms

Despite the fact that radiocesium concentrations in litter decreased over time during the 2014 to 2016 study period, they did not show a corresponding decrease in earthworms. To examine whether this was due to bioaccumulation, we studied the distribution of radiocesium in earthworms collected from Fukushima. Experiments on metabolism of radiocesium and autoradiography were performed in earthworms collected in 2016.

Although our findings indicated no evidence of radiocesium bioaccumulation in specific tissues or organs, we observed high radioactive contents in the digestive tract, suggesting that the high radiocesium concentrations in these earthworms are attributable to ingestion of highly contaminated organic matter.

It is well known that earthworms bioaccumulate heavy metal elements. Goswami et al. (2014) reported that Mn, Zn, Cu, and as accumulate in both of *Eisenia fetida* and *Lampito mauritii,* with an increase in metal-inducible metallothionein being a possible causal mechanism. However, in this study, autoradiograpic analysis gave no indication of radiocesium accumulation in earthworms (Chapter 4). Cesium is an alkali metal, with no affinity to specific body organs or tissues, and radiocesium distributes uniformly in the body of mammals (Moore and Comar, 1962).

This lack of accumulation is important from the viewpoint of radiation protection. The ICRP has issued recommendations for radiation protection of non-human biota (ICRP, 2008), in which 12 animals and plants, including earthworms, are specified as reference organisms for monitoring contamination and assessing the hazards to organisms living at or near the soil surface. The present findings indicate that the concentration of radiocesium in earthworms is a good indicator for contamination levels in leaf litter and surface soil, and that internal radiation exposure is uniform in the body.

Notably, however, the results presented here were derived from observations on only one family of epigeic earthworms (Megascolecidae), and thus it may be necessary to investigate other earthworm taxa, particularly those with trophic habits or physiologies that differ from those of this group. In addition, since the present study was carried out in earthworms collected during the summer season, it would be informative to investigate seasonal and regional variations, since habitats and physiological functions may also vary on temporal and spatial scale.

6.3 Absorbed dose rate and risk assessment in earthworms and spiders

Severe environmental contamination with radiocesium invevitably arouses public concern regarding the likelihood of radiation hazards, not only with respect to humans but also to wild animals and plants. Therefore, we estimated radiation doses and assessed potential risks in order to evaluate whether radiation poses a hazard to arthropods and earthworms. We accordingly found that total dose rate in the earthworms was 24.5 µGy/h (Table 5-1), with 96% of this load attributable to external exposure. For the Jorô spider, the total dose rate was 3.94 µGy/h (Table 5-2), with a large portion of this load again being due to external exposure.

For the purposes of radiation protection of non-human biota in natural ecosystems, the ICRP has established recommended sose rates for reference plants and animals, termed derived consideration reference levels (DCRLs). DCRLs include bands of dose rates with certain effects that have been reported or might be expected (ICRP, 2008). At present, the DCRLs for both earthworms and bees are within the range 10–100 mGy/day (Fig. 5-1). The rates estimated for earthworms and spiders in this study are considerably lower than these DCRLs, thereby indicating that adverse effects of direct radiation on these species are unlikely at present or in the future in Fukushima Prefecture.

However, researchers have observed certain morphological and functional changes or abnormalities in some wild animals and plants associated with the Fukushima accident. For example, Kubota et al. (2015) detected chromosomal aberration in the blood cells of wild rats, and Watanabe et al. (2015) observed morphological defects in native Japanese fir trees. Therefore, it is apparent that the FDNPP accident has affected the ecosystem of the immediate surroundings at least to some degree.

Ecosystems consists of a variety of organisms, including microbes, plants, and animals, interacting with one another, and it is possible that the effects of radiation on individual organisms differ from the effects at the ecosystem level. Although the radiation doses in earthworms and arthropods detected in this study were well below the levels at which obvious individual effects might be expected, it is a possible that these animals may experience indirect effects of radiation exposure caused by the FDNPP accident, due to their relationships with other ecosystem biota. Accordingly, comprehensive and continuous surveillance and investigation are necessary to effectively evaluate radiation doses and possible hazards in these non-human biota.

6.4 Present and future status of radiation in the Fukushima environment

The FDNPP accident caused widespread and serious environmental contamination with radioactive materials in Fukushima Prefecture and its vicinity, particularly by the major radionuclides ^{134}Cs and ^{137}Cs. Following the necessary decontamination measures, recovery and reconstruction are now progressing by the continuous and devoted efforts of local residents and related organizations. Ambient dose equivalent rates of radiation exposure for residents have been decreasing steadily in both urban areas and agricultural fields, due to physical decay of radiocesium as well as the artificial decontamination treatments. Kinase et al. (2014) have reported respective ecological half-lives of 0.84 y and 1.15 y in urban areas and agricultural fields based on ambient dose equivalent rates. In contrast, decreases in the ambient dose rate in forests and non-cultivated fields have been less pronounced, since active decontamination procedures were not applied in these regions. As is shown in Chapter 2, the decreases in ambient radiation dose are mainly due to the physical decay of radiocesium.

Recently, the Japanese government has begun the decontamination of the highly contaminated area where residents have yet to be permitted to return. Officials have also begun investigating efficient decontamination methods for forest areas, where radiation levels remain high and people are not allowed to enter. Since approximately 71% of the Fukushima Prefecture area is forested, its decontamination is essential for the region to fully recover. In order to accomplish this, efficient and economical decontamination methods must be developed and implemented based on a comprehensive knowledge about the behavior of radiocesium in the forest environment.

In this study, we have determined the behavior of radiocesium in arthropods and earthworms in a hilly and mountainous area of Fukushima, and identified trophic pathways for its transfer. Research based on the biological patterns of radiocesium will be beneficial in terms of gaining a better understanding of the mechanisms underlying the long-term environmental behavior of this radionuclide, and will contribute to the development of efficient and economical decontamination methods for Fukushima's revitalization.

7. Acknowledgements

First and foremost I would like to express my sincere gratitude to Professor. Sentaro Takahashi, who accommodated me in his laboratory in 2014 and provided continuous supported throughout my 5 years there. His direction and guidance helped me in all aspects of my research, and without which I could not have completed the study. I am very fortunate to have been given to opportunity to gain such valuable experience under his supervision.

I would like to express my sincere appreciation to Associate Professor Tomoyuki Takahashi for his practical advice, valuable discussions, and continuous encouragement. His guidance helped me throughout both the period of research and the time spent writing this thesis.

I would like also like to express my sincere appreciation to Professor Kanehiro Kitayama and Associate Professor Masahiro Osakabe for reviewing my thesis and providing insightful comments that broadened the scope of the thesis from various perspectives.

I am grateful to Professor Tarô Adati for providing me with the opportunity to conduct field studies in Fukushima in the wake of the nuclear accident in 2011. Without him, this study could not have been started. His determination and motivation gave me considerable inspiration for the research.

I would like to thank Drs. Kinashi Yuko, Hiroshi Yashima, and Hidehito Nakamura for their encouragement and valuable comments on my study.

I would like to thank Dr. Tadatoshi Kinouchi who assisted me in conducting laboratory work. He was invariably on hand to help me with my studies and gave me insightful suggestions for the research. I would also like to thank Drs. Satoshi Fukutani, Takumi Kubota, Takeshi Saito, and Maiko Ikegami for their valuable support throughout the study.

I would like to thank Drs. Tetsuji Imanaka and Manabu Fukumoto for providing opportunities to present information and write about the impact of the Fukushima accident on non-human biota.

I would like to thank S. Matuoka, a resident of Iitate, and M. Kamino for permitting access to sampling sites, and also thank the following members of the Department of International Agricultural Development, Tokyo University of Agriculture, for their assistance in field sampling: H. Shima, A. Kudo, Y. Kikuchi, E. Haneda, R Hirakawa, K. Hoshino, R. Maeda, I. Tôma, T. Naruoka, G. Tanaka, A. Kakuta, W. Kinjo, K. Hatakeyama, K. Hoshino, I. Touma, T. Naruoka, G. Tanaka, A. Kakuta, W. Kinjo, S. Takeda, K. Hakomori, Y. Hoshino, R. Ishino, and K. Kitada. I also thank K. Shoji of the Isotope Center, Tokyo University of Agriculture, for assisting in the surveys.

I would like to thank my current lab colleagues Kayoko Iwata and Rui Akayama, and former lab members Tomoyuki Ikawa, Naoki Takashima, Natsuya Yokomizo, Yuki Hattori, and Philip Long Nguyen, for their support during my time in the laboratory. I would also like to thank Naho Yoshida and Momoyo Ikeda for their support in the laboratory.

I would like to thank Keiko Fujiwara, Daisuke Maki, and Yuto Iinuma from the Kyoto University Institute for Integrated Radiation and Nuclear Science, who provided assistance and advice regarding the measurements and equipment used during this study.

The research described in this thesis was financially supported by the East Japan Assistance Project organized by the Tokyo University of Agriculture, and JSPS KAKENHI Grant Number JP16K08134 and a Grant-in-aid for JSPS fellows (16J10112).

8. References

Adachi, K., Kajino, M., Zaizen, Y., Igarashi, Y., 2013. Emission of spherical cesium-bearing particles from an early stage of the Fukushima nuclear accident. Sci. Rep. 3, 2554.

Allaye-Chan, A. C., White, R. G., Holleman, D. F., Russell, D. E., 1990. Seasonal concentrations of cesium-137 in rumen content, skeletal muscles and feces of caribou from the Porcupine herd: lichen ingestion rates and implications for human consumption. Rangifer, 10(3), 17-24.

Akimoto, S., 2014. Morphological abnormalities in gall-forming aphids in a radiation-contaminated area near Fukushima Daiichi: selective impact of fallout? Ecol. Evol. 4, 355-369.

Ando, K., 1996. Emergence factor and dispersal ability of rice grasshopper. Competition summary of Japanese Society of Applied Entomology and Zoology, No.40:70. (in Japanese).
https://ci.nii.ac.jp/els/contents110001088236.pdf?id=ART0001244697

Ando, Y., Yamashiro, C., 1993. Outbreaks and delayed hatching after hibernation in the rice grasshopper, *Oxya yezoensis* Shiraki (Orthoptera: Catantopidae). Appl. Entomol. Zool. 28(2), 217-225.

Auvinen, A., Lehtinen, K. E., Enriquez, J., Jokiniemi, J. K., Zilliacus, R., 2000. Vaporisation rates of CsOH and CsI in conditions simulating a severe nuclear accident. J. Aerosol Sci. 31(9), 1029-1043.

Ayabe, Y., Kanasashi, T., Hijii, N., Takenaka, C., 2015. Monitoring radiocesium contamination of the web spider *Nephila clavata* (Nephilidae: arachnida) in Fukushima forests. J. Jpn. For. Soc. 97, 70-74.

Baldwin, W.F., 1968. Increased yield of gamma-induced eye colour mutations from chronic versus acute exposures in *Dahlbominus*. In: Isotopes and Radiation in Entomology; IAEA, Vienna, pp. 365-375.

Bonkowski, M., Schaefer, M., 1997. Interactions between earthworms and soil protozoa: a trophic component in the soil food web. Soil Biol. Biochem. 29, 499–502.

Bonkowski, M., Griffiths, B.S., Ritz, K., 2000. Food preferences of earthworms for soil fungi. Pedobiologia 44, 666–676.

Bouché, M.B., 1977. Stratégies lombriciennes. In: Lohm, U., Persson, T. (Eds.), Soil

Organisms as Components of Ecosystems. Biol. Bull. 25, 122-132.
Brown, G.G., 1995. How do earthworms affect microflora and faunal community diversity? Plant and Soil 170, 209–231.
Brown, J. E., Alfonso, B., Avila, R., Beresford, N. A., Copplestone, D., Pröhl, G., Ulanovsky, A., 2008. The ERICA tool. J. Environ. Radioact. 99(9), 1371-1383.
Brown, S.L., Bell, J.N.B., 1995. Earthworms and radionuclides, with experimental investigations on the uptake and exchangeability of radiocaesium. Environ. Pollut. 88, 27–39.
Brückmann, A., Wolters, V., 1994. Microbial immobilization and recycling of ^{137}Cs in the organic layers of forest ecosystems: relationship to environmental conditions, humification and invertebrate activity. Sci. Total Environ. 157, 249–256.
Carmona D.M., Menalled F.D. Landis D.A., 1999. Gryllus pennsylvanicus (Orthoptera: Gryllidae): laboratory weed seed predation and within field activity–density. J. Econ. Entomol. 92, 825–829.
Cort M. de, Dubois G, Fridman S.D., Germenchuk M.G., Izrael Y.A., Janssens A, et al. Atlas of cesium deposition on Europe after the Chernobyl accident. EUR Report Nr. 16733. Brussels-Luxemburg: Office for Official Publications of the European Communities; ECSC-EEC-EAEC; 1998.
Doube, B.M., Schmidt, O., Killham, K., Correll, R., 1997. Influence of mineral soil on the palatability of organic matter for lumbricid earthworms: a simple food preference study. Soil Biol. Biochem. 29, 569–575.
Dreicer, M., Aarkog, A., Alexakhin, R., Anspaugh, L., Arkhipov, N. P., Johansson, K. J., 1996. Consequences of the Chernobyl accident for the natural and human environments (No. UCRL-JC--125028). Lawrence Livermore National Lab.
Edwards, C.A., Fletcher, K.E., 1988. Interactions between earthworms and microorganisms in organic-matter breakdown. Agric. Ecosyst. Environ. 24, 235–247.
ElEla, S.A., ElSayed, W., Nakamura, K., 2010. Mandibular structure, gut contents analysis and feeding group of orthopteran species collected from different habitats of Satoyama area within Kanazawa City. Jpn. J. Threat. Taxa 2, 849-857.
Endo, S., Tanaka, K., Kajimoto, T., Thanh, N. T., Otaki, J. M., Imanaka, T., 2014. Estimation of β-ray dose in air and soil from Fukushima Daiichi Power Plant accident. J. Radiat. Res. 55(3), 476-483.
England, T. R., & Rider, B. F., 1995. Evaluation and compilation of fission product yields 1993 (No. LA-SUB--94-170). Los Alamos National Lab.
Evangeliou, N., Balkanski, Y., Cozic, A., Møller, A.P., 2013. Global transport and

deposition of ^{137}Cs following the Fukushima nuclear power plant accident in Japan: emphasis on Europe and Asia using high-resolution model versions and radiological impact assessment of the human population and the environment using interactive tools. Environ. Sci. Technol. 47, 5803-5812.
Fesenko, S., Sanzharova, N., Tagami, K., 2009. Evaluation of Plant Contamination with Time. Quantification of radionuclide transfer in terrestrial and freshwater environments for radiological assessments. IAEA-Tecdoc-1616.
Fisher, N. S., Beaugelin-Seiller, K., Hinton, T. G., Baumann, Z., Madigan, D. J., Garnier-Laplace, J., 2013. Evaluation of radiation doses and associated risk from the Fukushima nuclear accident to marine biota and human consumers of seafood. Proc. Natl. Acad. Sci. 110(26), 10670-10675.
Fujii, K., Ikeda, S., Akama, A., Komatsu, M., Takahashi, M., Kaneko, S., 2014. Vertical migration of radiocesium and clay mineral composition in five forest soils contaminated by the Fukushima nuclear accident. Soil Sci. Plant Nutr. 60 (6), 751–764.
Fujiwara, K., Takahashi, T., Nguyen, P., Kubota, Y., Gamou, S., Sakurai, S., Takahashi, S., 2015. Uptake and retention of radio-caesium in earthworms cultured in soil contaminated by the Fukushima nuclear power plant accident. J. Environ. Radioact. 139, 135–139.
Fukushima Prefectural Government, 2010. The Strategy for the Promotion of Depopulated Hilly and Mountainous Area in Fukushima Prefecture. Fukushima Prefectural Government, Fukushima.
Fukushima Prefectural Government, 2017. Forest and forestry statistics (accessed 20 Nov. 2018). https://www.pref.fukushima.lg.jp/uploaded/attachment/262415.pdf.
Fukushima Prefectural Government, 2018. Ttansition of evacuation designated zones. (Accessed 20 Nov 2018) http://www.pref.fukushima.lg.jp/site/portal-english/en03-08.html
Fuma, S., Ihara, S., Kawaguchi, I., Ishikawa, T., Watanabe, Y., Kubota, Y., Soeda, H., 2015. Dose rate estimation of the Tohoku hynobiid salamander, Hynobius lichenatus, in Fukushima. J. Environ. Radioact. 143, 123-134.
Garnier-Laplace, J., Beaugelin-Seiller, K., Hinton, T. G., 2011. Fukushima wildlife dose reconstruction signals ecological consequences.
Goor, F., Thiry, Y., 2004. Processes, dynamics and modelling of radiocaesium cycling in a chronosequence of Chernobyl-contaminated Scots pine (Pinus sylvestris L.) plantations. Sci. Tot. Environ. 325(1-3), 163-180.

Goswami, L., Sarkar, S., Mukherjee, S., Das, S., Barman, S., Raul, P., Bhattacharya, S. S., 2014. Vermicomposting of tea factory coal ash: metal accumulation and metallothionein response in Eisenia fetida (Savigny) and Lampito mauritii (Kinberg). Biores. Technol. 166, 96-102.

Haffner, R. L., Howells, G. P., Lauer, G. R., Hirshfield, H.I., 1973. Effects of power plant operation on Hudson River estuary microbiota. In: Nelson, D.J.(Ed.), Radionuclides in Ecosystem. Proceedings of the Third National Symposium on Radioecology, 10-12 May 1971. (No. CONF-710501-P2). Oak Ridge, TN, pp. 619-629.

Hasegawa, M., Ito, M.T., Kaneko, S., Kiyono, Y., Ikeda, S., Makino, S.I., 2013. Radiocesium concentrations in epigeic earthworms at various distances from the Fukushima Nuclear Power Plant 6 months after the 2011 accident. J. Environ. Radioact. 126, 8–13.

Hasegawa, M., Kaneko, S., Ikeda, S., Akama, A., Komatsu, M., Ito, M.T., 2015. Changes in radiocesium concentrations in epigeic earthworms in relation to the organic layer 2.5 years after the 2011 Fukushima Dai-ichi Nuclear Power Plant accident. J. Environ. Radioact. 145, 95–101.

Heikens, A., Peijnenburg, W. J. G. M., Hendriks, A. J., 2001. Bioaccumulation of heavy metals in terrestrial invertebrates. Environ. Pollut. 113(3), 385-393.

Hendrichs, J., 2000. Use of the sterile insect technique against key insect pests. Sustainable Dev. Int. 2: 75-79.

Hertel-Aas, T., Oughton, D. H., Jaworska, A., Bjerke, H., Salbu, B., Brunborg, G., 2007. Effects of chronic gamma irradiation on reproduction in the earthworm Eisenia fetida (Oligochaeta). Radiat. Res. 168(5), 515-526.

Hiyama, A., Nohara, C., Kinjo, S., Taira, W., Gima, S., Tanahara, A., Otaki, J.M., 2012. The biological impacts of the Fukushima nuclear accident on the pale grass blue butterfly. Sci. Rep. 2, 570.

Hobbelen, P. H. F., Koolhaas, J. E., Van Gestel, C. A. M., 2006. Bioaccumulation of heavy metals in the earthworms Lumbricus rubellus and Aporrectodea caliginosa in relation to total and available metal concentrations in field soils. Environ. Pollut. 144(2), 639-646.

IAEA (International Atomic Energy Agency), 2000. Generic Procedures for Assessment and Response during a Radiological Emergency. IAEA-Tecdoc-1162.

IAEA (International Atomic Energy Agency). 2006. Environmental Consequences of the Chernobyl Accident and their Remediation: Twenty Years of Experience.

IAEA (International Atomic Energy Agency), 2015a. The Fukushima Daiichi Accident.

Technical Volume 1/5. Description and Context of the Accident.
IAEA (International Atomic Energy Agency), 2015b. The Fukushima Daiichi Accident. Technical Volume 4/5. Description and Context of the Accident.
IAEA/IDIDAS, 2018. International Database on Insect Disinfestation and Sterilization. http://www-ididas.iaea.org/ididas/
Ichihara, M., Inagaki, H., Matsuno, K., Saiki, C., Yamashita, M., Sawada, H., 2012. Postdispersal seed predation by Teleogryllus emma (Orthoptera: Gryllidae) reduces the seedling emergence of a non‐native grass weed, Italian ryegrass (Lolium multiflorum). Weed Biol. Manag. 12(3), 131-135.
ICRP (International Commission on Radiological Protection), 2008. Environmental Protection - the Concept and Use of Reference Animals and Plants. ICRP Publication 108. Ann. ICRP 38 (4–6).
Imanaka, T., Hayashi, G., Endo, S., 2015. Comparison of the accident process, radioactivity release and ground contamination between Chernobyl and Fukushima-1. J. Radiat. Res. 56(suppl_1), i56-i61.
Ishizuka, K. 2015. Academic Study of earthworms Morphology, ecology, taxonomy and research methods of Japanese Earthworms (Genus *Pheretima s*. lat.). (in Japanese).
Jarvis, N.J., Taylor, A., Larsbo, M., Etana, A., Rosen, K., 2010. Modelling the effects of bioturbation on the re-distribution of ^{137}Cs in an undisturbed grassland soil. Eur. J. Soil Sci. 61 (1), 24–34.
Kaneyasu, N., Ohashi, H., Suzuki, F., Okuda, T., Ikemori, F., 2012. Sulfate aerosol as a potential transport medium of radiocesium from the Fukushima nuclear accident. Environ. Sci. Technol. 46(11), 5720-5726.
Kashimura, T. 1984. Natural forest around lake Inawashiro. Nature of lake Inawashiro. 33-39. (in Japanese).
Kashparov, V. A., Lundin, S. M., Zvarych, S. I., Yoshchenko, V. I., Levchuk, S. E., Khomutinin, Y. V., Protsak, V. P., 2003. Territory contamination with the radionuclides representing the fuel component of Chernobyl fallout. Sci. Total Environ. 317(1-3), 105-119.
Kålås, J. A., Bretten, S., Byrkjedal, I., Njåstad, O., 1994. Radiocesium (^{137}Cs) from the Chernobyl reactor in Eurasian woodcock and earthworms in Norway. J. Wildlife Manage. 141-147.
Kato, H., Onda, Y., Gomi, T., 2012. Interception of the Fukushima reactor accident-

derived ^{137}Cs, ^{134}Cs and ^{131}I by coniferous forest canopies. Geophys. Res. Lett. 39, 1–6.

Kato, H., Onda, Y., Saidin, Z. H., Sakashita, W., Hisadome, K., Loffredo, N., 2018. Six-year monitoring study of radiocesium transfer in forest environments following the Fukushima nuclear power plant accident. J. Environ. Radioact. In press.

Kinase, S., Takahashi, T., Sato, S., Sakamoto, R., Saito, K., 2014. Developmentof prediction models for radioactive caesium distribution within the 80-km radius of the Fukushima Daiichi nuclear power plant. Radiat. Protect. Dosim. 160, 318–321.

Krivolutzkii, D. A., Pokarzhevskii, A. D., 1992. Effects of radioactive fallout on soil animal populations in the 30 km zone of the Chernobyl atomic power station. Sci. Total. Environ. 112(1), 69-77.

Krivolutzkii, D.A., Pokarzhevskii, A.D., Viktorov, A.G., 1992. Earthworm populations in soils contaminated by the chernobyl atomic power station accident, 1986–1988. Soil Biol. Biochem. 24 (12), 1729–1731.

Kruyts, N., Delvaux, B., 2002. Soil organic horizons as a major source for radiocesium biorecycling in forest ecosystems. J. Environ. Radioact. 58(2-3), 175-190.

Kryshev, I.I., Kryshev, A.I., Sazykina, T.G., 2012. Dynamics of radiation exposure to marine biota in the area of the Fukushima NPP in March-May 2011. J. Environ. Radioact. 114, 157-161.

Koarashi, J., Atarashi-Andoh, M., Matsunaga, T., Sato, T., Nagao, S., Nagai, H., 2012. Factors affecting vertical distribution of Fukushima accident-derived radiocesium in soil under different land-use conditions. Sci. Total Environ. 431, 392–401.

Koarashi, J., Atarashi-Andoh, M., Takeuchi, E., Nishimura, S., 2014. Topographic heterogeneityeffect on the accumulation of Fukushima-derived radiocesium on forest floor driven by biologically mediated processes. Sci. Rep. 4, 6853.

Kubota, Y., Takahashi, H., Watanabe, Y., Fuma, S., Kawaguchi, I., Aoki, M., Ishikawa, T., 2015. Estimation of absorbed radiation dose rates in wild rodents inhabiting a site severely contaminated by the Fukushima Dai-ichi nuclear power plant accident. J. Environ. Radioact. 142, 124-131.

Kubota, Y., Tsuji, H., Kawagoshi, T., Shiomi, N., Takahashi, H., Watanabe, Y., Kubota, M., 2015. Chromosomal aberrations in wild mice captured in areas differentially contaminated by the Fukushima Dai-Ichi Nuclear Power Plant accident. Environ. Sci.Technol. 49(16), 10074-10083.

Kuntner, M., Agnarsson, I., 2011. Phylogeography of a successful aerial disperser: the golden orb spider Nephila on Indian Ocean islands. BMC Evol. Biol. 11(1), 119.

Lavelle, P., Bignell, D., Lepage, M., Wolters, W., Roger, P., Ineson, P., Heal, O.W., Dhillion, S., 1997. Soil function in a changing world : the role of invertebrate ecosystem engineers. Eur. J. Soil Biol. 33, 159–193.

Lee, K.E., 1985. Earthworms: Their Ecology and Relationships with Soils and Land Use. Academic Press Inc.

Li, L., Xu, Z., Wu, J., Tian, G., 2010. Bioaccumulation of heavy metals in the earthworm Eisenia fetida in relation to bioavailable metal concentrations in pig manure. Biores. Tech. 101(10), 3430-3436.

Loffredo, N., Onda, Y., Kawamori, A., Kato, H., 2014. Modeling of leachable 137Cs in throughfall and stemflow for Japanese forest canopies after Fukushima Daiichi Nuclear Power Plant accident. Sci. Total Environ. 493, 701–707.

Lundgren J.G., Rosentrater K.A., 2007. The strength of seeds and their destruction by granivorous insects. Arthropod Plant Interact. 1, 93–99.

Ministry of Education, Culture, Sports, Science and Technology (MEXT), 2011. Extension Site of Distribution Map of Radiation Dose, etc.: Airborne Monitoring Results as of June 28, 2012 (5th + outside 80km) (Accessed24 Nov 2018). https://ramap.jmc.or.jp/map/eng/#lat=37.28677324902984&lon=141.17637270859322&z=9&b=std&t=air&s=8,0,0,0&c=20120628_cstotal

Ministry of Education, Culture, Sports, Science and Technology (MEXT), 2011. Extension Site of Distribution Map of Radiation Dose, etc.: Airborne Monitoring Results as of April 29, 2011 (1st) (Accessed 24 Nov 2018). https://ramap.jmc.or.jp/map/eng/#lat=37.28458799999977&lon=140.5831109999977&z=9&b=std&t=air&s=17,0,0,0&c=20111013_cstotal.

Mitsuhashi, J., 2003. Traditional entomophagy and medicinal use of insects in Japan. Les Insectes dans la tradition orale-Insects in oral literature and traditions, XXX press.,357-365.

Miyashita, T., Takada, M., Shimazaki, A., 2003. Experimental evidence that aboveground predators are sustained by underground detritivores. Oikos, 103(1), 31-36.

Møller, A.P., Nishiumi, I., Suzuki, H., Ueda, K., Mousseau, T.A., 2013. Differences in effects of radiation on abundance of animals in Fukushima and Chernobyl. Ecol. Indic. 24, 75-81.

Moore, W., Comar, C. L., 1962. Absorption of caesium 137 from the gastro-intestinal tract of the rat. Int. J. Radiat. Biol. Relat. Stud. Phys. Chem. Med. 5(3), 247-254.

Murakami, M., Ohte, N., Suzuki, T., Ishii, N., Igarashi, Y., Tanoi, K., 2014. Biological proliferation of cesium-137 through the detrital food chain in a forest ecosystem in Japan. Sci. Rep. 4, 3599.

Nakanishi, T., Matsunaga, T., Koarashi, J., Atarashi-Andoh, M., 2014. ^{137}Cs vertical migration in a deciduous forest soil following the Fukushima Dai-ichi Nuclear Power Plant accident. J. Environ. Radioact. 128, 9–14.

Nakao, A., Thiry, Y., Funakawa, S., Kosaki, T. 2008. Characterization of the frayed edge site of micaceous minerals in soil clays influenced by different pedogenetic conditions in Japan and northern Thailand. Soil Sci. Plant Nutr. 54(4), 479-489.

Neilson, R., Boag, B., 2003. Feeding preferences of some earthworm species common to upland pastures in Scotland. Pedobiologia 47, 1–8.

Niizato, T., Abe, H., Mitachi, K., Sasaki, Y., Ishii, Y., Watanabe, T., 2016. Input and output budgets of radiocesium concerning the forest floor in the mountain forest of Fukushima released from the TEPCO's Fukushima Dai-ichi nuclear power plant accident. J. Environ. Radioact. 161, 11–21.

Ochiai, K., Hayama, S. I., Nakiri, S., Nakanishi, S., Ishii, N., Uno, T., Omi, T., 2014. Low blood cell counts in wild Japanese monkeys after the Fukushima Daiichi nuclear disaster. Sci. Rep. 4, 5793.

Oste, L. A., Dolfing, J., Ma, W. C., Lexmond, T. M., 2001. Cadmium uptake by earthworms as related to the availability in the soil and the intestine. Environ. Toxicol. Chem. 20(8), 1785-1791.

Polis, G.A., Strong, D.R., 1996. Food web complexity and community dynamics. Am. Nat. 147, 813-846.

R Core Team, 2013. R: A Language and Environment for Statistical Computing. R Foundation for Statistical Computing, Vienna, Austria ISBN 3-900051-07-0. http://www.R-project.org/.

Reichle, D. E., Witherspoon, J. P., Mitchell, M. J., Styron, C. E., 1972. Effects of beta-gamma radiation of earthworms under simulated-fallout conditions. In: Proceedings of Survival of Food Crops and Livestock in the Event of Nuclear War. AEC Symposium Series 24. Brookhaven National Laboratory, 1970. CONF-700909 US Atomic Energy Commission, Washington, DC, pp. 527-534.

Riordan, D.F., 1964. Effect of continuous low-level gamma-irradiation on successive generations of *Dahlbominus fuscipennis* (*zett.*) (Hymenoptera: Eulophidae). Chromosoma 42, 685-688.

Robinson, MH., Robinson, B., 1973. Ecology and behavior of the giant wood spider Nephila maculate (Fabricius): in New Guinea. Smithson. Contrib. Zool. 149, 1-76.

Romijn, C. A. F. M., Luttik, R., Slooff, W., Canton, J. H., 1991. Presentation of a general algorithm for effect-assessment on secondary poisoning. II Terrestrial food chains. RIVM Rapport 679102007.

Saito, K., Petoussi-Henss, N., 2014. Ambient dose equivalent conversion coefficients for radionuclides exponentially distributed in the ground. J. Nucl. Sci. Technol. 51(10), 1274-1287.

Saito, K., Tanihata, I., Fujiwara, M., Saito, T., Shimoura, S., Otsuka, T., Kinouchi, N., 2015. Detailed deposition density maps constructed by large-scale soil sampling for gamma-ray emitting radioactive nuclides from the Fukushima Dai-ichi Nuclear Power Plant accident. J. Environ. Radioact. 139, 308-319.

Sheppard, S.C., Evenden, W.G., Cornwell, T.C., 1997. Depuration and uptake kinetics of I, Cs, Mn, Zn and Cd by the earthworm (Lumbricus terrestris) in radiotracer-spiked litter. Environ. Toxicol. Chem. 16 (10), 2106–2112.

Shimazaki, A., Miyashita, T., 2005. Variable dependence on detrital and grazing food webs by generalist predators: aerial insects and web spiders. Ecography 28, 485-494.

Steiner, M., Linkov, I., Yoshida, S., 2002. The role of fungi in the transfer and cycling of radionuclides in forest ecosystems. J. Environ. Radioact. 58, 217–241.

Strand, P., Aono, T., Brown, J.E., Garnier-Laplace, J., Hosseini, A., Sazykina, T., Steenhuisen, F., Vives i Batlle, J., 2014. Assessment of Fukushima-derived radiation doses and effects on wildlife in Japan. Environ. Sci. Technol. Lett. 1, 198-203.

Suzuki, J., Egami, N., 1983. Mortality of the Earthworms, Eisenia foetida, after γ-irradiation at Different Stages of Their Life History. J. Radiat. Res. 24(3), 209-220.

Tagami, K., 2012. Transfer of radionuclides to the higher plants through direct deposition and root uptake pathways. Radioisotopes, 61(5), 267-279. (in Japanese).

Takeda, A., Tsukada, H., Nakao, A., Takaku, Y., Hisamatsu, S. I., 2013. Time-dependent changes of phytoavailability of Cs added to allophanic Andosols in laboratory cultivations and extraction tests. J. Environ. Radioact. 122, 29-36.

Takeda, H., Ichimura, T., 1983. Feeding attributes of four species of Collembola in a pine forest soil. Pedobiol.

Takada, M., Yamada, T., Takahara, T., Endo, S., Tanaka, K., Kajimoto, T., Okuda, T., 2017. Temporal changes in vertical distribution of 137Cs in litter and soils in mixed deciduous forests in Fukushima. Japan. J. Nucl. Sci. Technol 54 (4), 452–458.

Teramage, M.T., Onda, Y., Kato, H., Gomi, T., 2014. The role of litterfall in transferring Fukushima-derived radiocesium to a coniferous forest floor. Sci. Total Environ. 490,

430–439.
Thiry, Y., Garcia-Sanchez, L., Hurtevent, P., 2016. Experimental quantification of radiocesium recycling in a coniferous tree after aerial contamination: Field loss dynamics, translocation and final partitioning. J. Environ. Radioact. 161, 42-50.
Thomas, R. G., Thomas, R. L., 1967. Long Term Whole-Body Retention After High Level CESIUM-137 Administration to Rats (No. LF-35). Lovelace Foundation for Medical Education and Research Albuquerque Nm.
Tyler, A.N., Carter, S., Davidson, D.A., Long, D.J., Tipping, R., 2001. The extent and significance of bioturbation on ^{137}Cs distributions in upland soils. Catena 43 (2), 81–99.
Uchida, T., Kaneko, N., Ito, M.T., Futagami, K., Sasaki, T., Sugimoto, A., 2004. Analysis of the feeding ecology of earthworms (Megascolicidae) in Japanese forests using gut content fractionation and delta ^{15}N and delta ^{13}C stable isotope natural abundances. Appl. Soil Ecol. 27, 153–163.
UNSCEAR (United Nations Scientific Committee on the Effects of Atomic Radiation), 1988. Exposure from the Chernobyl accident (annex D).
UNSCEAR (United Nations Scientific Committee on the Effects of Atomic Radiation), 1996. Sources, Effects and Risks of Ionizing Radiation (Report to the General Assembly).
UNSCEAR (United Nations Scientific Committee on the Effects of Atomic Radiation), 2000. Exposures and effects of the Chernobyl accident (annex J).
UNSCEAR (United Nations Scientific Committee on the Effects of Atomic Radiation), 2008. Sources and effects of ionizing radiation (annex D).
UNSCEAR (United Nations Scientific Committee on the Effects of Atomic Radiation), 2013. Sources and effects of ionizing radiation (annex A).
Vinichuk, M. M., Johanson, K. J., Rosen, K., Nilsson, I., 2004. Role of the fungal mycelium in the retention of radiocaesium in forest soils. J. Environ. Radioact. 78(1), 77-92.
Vreysen, M.J.B. 2001. Principles of area-wide integrated tsetse fly control using the sterile insect technique. Med. Trop. 61: 397-411
Watanabe, Y., Kubota, M., Hoshino, J., Kubota, Y., Maruyama, K., Fuma, Yoshida, S., 2015. Morphological defects in native Japanese fir trees around the Fukushima Daiichi Nuclear Power Plant. Sci. Rep. 5, 13232.
WHO (Worlf Health Organization), 2006. Health Effects of the Chernobyl Accident and

Special Health Care Programmes.

WHO (Worlf Health Organization), 2016. 1986-2016 CHERNOBYL at 30 An update.

Yamashita, J., Enomoto, T., Yamada, M., Ono, T., Hanafusa, T., Nagamatsu, T., Yamamoto, Y., 2014. Estimation of soil-to-plant transfer factors of radiocesium in 99 wild plant species grown in arable lands 1 year after the Fukushima 1 Nuclear Power Plant accident. J. Plant res., 127(1), 11-22.

Yoshida, S., Muramatsu, Y., Dvornik, A. M., Zhuchenko, T. A., Linkov, I., 2004. Equilibrium of radiocesium with stable cesium within the biological cycle of contaminated forest ecosystems. J. Environ. Radioact. 75(3), 301-313.

Yoshihara, T., 2017. Leaf Ecology and Radiocesium Contamination in Trees/Forests. In Plant Ecology-Traditional Approaches to Recent Trends. InTech.

Zhang, Z. Q., 2011. Animal biodiversity: An introduction to higher-level classification and taxonomic richness. Zootaxa, 3703(1), 5-11.